Report from the ICD-2 Research Program Task Force.

Sept XXth 2009.

1. Introduction:

In April of 2009 the Fermilab directorate charged a task force of accelerator physicists and experimental physicists to explore the opportunities and challenges presented by an alternative design to the Project-X accelerator. The first baseline design of the Project-X accelerator is described in the Initial Configuration Document (ICD) [1]. The charge for the task force can be found in Appendix-I and the task force membership can be found in Appendix-II. The task force met three times in May of 2009 and prepared an interim report that was presented to the Fermilab Physics Advisory Committee (PAC) in Aspen Colorado on June 24th. The response of the Fermilab PAC to the interim report can be found in Appendix-III. The PAC found the research potential of the alternative design to be high and consequently advised that the two accelerator designs be referred to as ICD-1, and IDC-2 for the previously referred to "alternative design".

The research program for Project-X is described in the "Golden Book" [2] which was developed during the 2008 Project-X workshops. The broad research program described in the Golden Book includes long-baseline neutrino experiments, neutrino interaction experiments, quark flavor Tevatron fixed target experiments (Appendix IV), ultra-rare muon and kaon decay experiments and experiments driven by anti-protons (Appendix V) from the Fermilab anti-proton complex. The long-baseline neutrino experiments and rare-decay experiments benefit most directly from the high proton beam power afforded by Project-X. This beam power presents simultaneously the promise of extraordinary physics reach and the substantial accelerator physics challenge of generating and handling enormous beam power.

The initial baseline design (ICD-1) of the Project-X accelerator complex can generate and handle the beam power required for the long-baseline neutrino program, however the high beam power available at 8 GeV is not readily useable by the rare-decay experiments. Further, the auxiliary accelerator concepts developed to handle and condition 8 GeV beam power for near-term muon experiments [3] does not scale well with increasing beam power and precludes the use of the Debuncher and Accumulator for the anti-proton research program described in the Golden Book.

The accelerator physics challenge presented by the ICD-1 in serving the long-baseline neutrino program and rare-decay program (and more broadly the full Golden Book research program) has motivated consideration of the ICD-2 alternative design. The ICD-2 is based on a 2 GeV Continuous Wave (CW) linac, and its impact on the Project-X research program is the subject of this report. As with the ICD-1 the ICD-2

can readily drive the long-baseline neutrino program, hence this report focuses on how the ICD-2 can drive the Project-X rare-decay research program.

This report outlines an accelerator architecture where a 2 GeV CW proton linac directly drives next generation rare decay programs. This scheme is the basis of ICD-2 and is a significant departure from the Project-X ICD-1 architecture. The findings of this report serve as an exploration of a 2 GeV-driven research program and more broadly the research program of the Fermilab accelerator complex other than neutrino physics.. The cost and schedule of the ICD-2 accelerator concept is discussed in a parallel document [XX].

1.1 Rare Decay Experiment Accelerator Requirements of the Proton Complex:

(Adapted from the Project-X Golden Book, ver. 1, Feb 3, 2008.)

The next generation of rare-decay experiments require kaon and muon beams of extraordinary quality. These experiments operate at the intensity frontier, where conventional decay and interaction processes can conspire in a high-rate environment to mimic the sought-after rare decay signatures. The principal weapon to control these backgrounds is the partnership of detectors that deliver excellent time resolution with high duty-factor beams which minimize the instantaneous rates that the detectors must face. Project-X is an exceptional opportunity to build a high intensity proton beam complex with nearly 100% duty factor and high availability (nominally 5000 hours per year). The joint potential of high duty factor and high availability would make the Fermilab complex a unique resource for rare-decay experiments.

Both the muon and kaon rare decay programs could have Phase I operation before the high-power Project X era (Phase II). A conceptual scheme has been developed to establish the required RF structure for Phase-I operation of the Mu2e and (g-2) experiments with an evolution of the existing Accumulator and Debuncher complex. These schemes are described in some detail in the Mu2e and (g-2) proposals [3]. The proton beam RF train requirements for the kaon and muon programs are listed below in Table 1.

	Train Frequency	Pulse Width (nanoseconds)	Inter-Pulse Extinction
Kaon experiments	20-30 MHz	<0.2	10^{-3}
Muon conversion experiment	0.5-1.0 MHz	<100	10^{-9*}
$\mu \rightarrow e\gamma$ & $\mu \rightarrow eee$ experiments	80-300 MHz	<0.2	---
Muon g-2 experiment	30-100 Hz	50	---

*muon conversion extinction is achieved by a combination of extinction in the circulating beam/extraction and in an external device in the proton beam transport

Table 1: RF train requirements for the kaon and muon rare decay programs.

2. Summary of Project-X accelerator R&D and Issues

2.1 Update on Fermilab Accelerator Complex R&D since the Golden Book (v1):

i) Ongoing accelerator upgrades should allow the Booster to accelerate $4x10^{12}$ protons (4 Tp) to 8 GeV (kinetic) at a 15-Hz cycle rate. This corresponds to a total beam power of 77 kW. Of this 50 kW is required for NOvA, leaving ~25 kW for other Phase-I applications (such as rare decays).

ii) The Recycler ring was determined to be unfavorable for a resonant slow extraction scheme mainly due to its small transverse aperture, large circumference (for an 8-GeV ring) and inflexible permanent-magnet lattice.

iii) The bunch structure for the Mu2e experiment (Table 1) can be provided by a resonant slow extraction from the Debuncher ring, which has a factor of 6 smaller circumference than the Recycler and a factor of 6 larger transverse aperture. The Mu2e experiment requires about 25 kW of protons. Higher beam power (and thus a higher muon flux) may be accommodated by the present detector design although the ultimate capabilities of the slow extraction from the Debuncher in the Mu2e scenario have not yet been studied exhaustively. One can argue that the beam power during the extraction will be limited by: uncontrolled beam losses (i.e. the 1 W/m loss limit), extraction inefficiencies because of the space charge, and tune ripple and momentum spread. From scaling considerations it is thought that beam power limit for the Mu2e scenario lies somewhere between 50 and 200 kW.

iv) The bunch structure for the kaon experiments in Phase-I would also require a resonant slow extraction. However, such a scenario was not yet seriously considered, as priority was given to developing the Mu2e and g-2 proposals. It is however clear that meeting the pulse width (aka bunch length) requirements for Kaon experiments would be quite challenging. Nominally, the Fermilab Booster and the MI operate with a 53-MHz bunch structure, which is close to Kaon train frequency requirements. However, the nominal bunch length is 1-2 ns – a factor of 10 longer than required. Since for a given longitudinal emittance the bunch length scales inversely with the fourth power of RF cavity voltage, reducing the bunch length by a factor of 10 would require substantial upgrades to the RF systems.

2.2 Summary of Phase-I opportunities and constraints:

Mu2e

Opportunities:

- Bunch structure can be met by employing the existing Recycler and Accumulator rings for re-bunching and the Debuncher ring for slow extraction.
- Ultimate extracted proton beam power is likely limited to 50-200 kW.

Constraints:

- Kaon, g-2, anti-proton experiments cannot operate simultaneously with the Mu2e experiment. Beam time per experiment will have to be portioned through program planning.

g-2

Opportunities:

- Bunch structure can be met by employing the existing Recycler ring. It also utilizes the anti-proton source target, AP-2 line and Debuncher but does not require decommissioning of the anti-proton source.

Constraints:

- Kaon, Mu2e, anti-proton experiments cannot operate simultaneously with the g-2 experiment. Beam time per experiment will have to portioned through program planning.
- The intent of the experiment to use the anti-proton source infrastructure has a time conflict with the Mu2e experiment expected to start data acquisition in 2016.

Kaons

- Unlikely to meet the bunch requirements of the neutral kaon decay experiment (proton ping timing σ<200 psec) with the existing 8-GeV complex.

Additional physics opportunities in rare decays and neutrinos can be pursued with a slow and/or fast extraction from the Tevatron. These opportunities are complementary to Phase-I program and are described in section 3.2.3 and Appendix III.

2.3 Summary of the Project-X Initial Configuration Document

The initial configuration design (ICD-1) of Project X [2] is designed to meet the following design criteria:

1. It must provide 2.1 MW of a single-turn extracted beam from the Main Injector at energies ranging from 60 to 120 GeV
2. It must provide 150 kW of 8-GeV beam to the Accumulator/Debuncher for the Mu2e experiment.
3. There must exist a plausible beam-power upgrade scenario (up to 4 MW at 8 GeV) for future neutrino and muon facilities.

The selected initial configuration consists of a pulsed 8-GeV linac capable of delivering up to $1.6\text{x}10^{14}$ protons to the Recycler in a 1.25 ms long pulses at a 2.5-Hz rate. The theoretical beam power available at 8 GeV is 0.5 MW. Of this, 150 kW (300 kW) is delivered to the Main Injector for acceleration to 120 (60) GeV and 150 kW is delivered to Mu2e in a specific bunch structure. The feasibility of slow extraction of such a beam power from the Debuncher was not studied. Figure 1 shows an accelerator timeline for a 60-GeV MI operation with a cycle of 0.8 seconds. A similar scenario also exists for a 120-GeV MI operation.

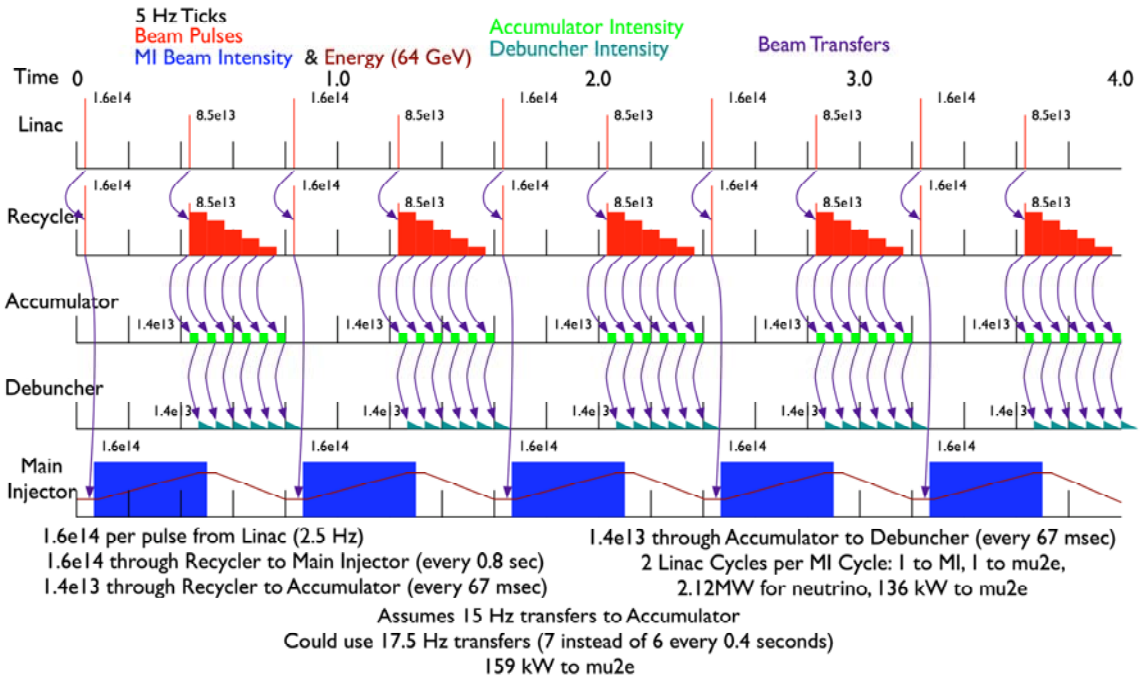

Figure 1: The Project X ICD-1 operational scenario for the MI running at 60 GeV.

The details of this design can be found in Ref. [1]. In summary, the ICD provides the following opportunities and constraints:

1. The 2.1-MW MI Neutrino program is supported.

2. Rare decays and precision measurements:
   - The Mu2e scenario is an evolution of the present Mu2e proposal [3]. The proposed power level of 150 kW is within the estimated range of Debuncher slow extraction beam power limits (50-200 kW) mentioned above. Since the slow extraction for the mu2e is outside of the ICD scope, the feasibility of extracting beam at this high power was not explored.
   - The g-2 scenario was not explored.
   - The Kaon experiment scenario was not explored. However, the ICD is unlikely to meet the bunch requirements in Table 1 for reasons described above.

3. A path to beam-power upgrade to 4 MW exists.

2.4 Summary of the ICD-2

The initial Project X ICD-1 design and goals were mainly driven by the Project X synergy with the ILC and the 2 MW operation of the MI for neutrino program. The details of operation with a slow extracted beam at 8 GeV were not considered in the Initial Conceptual Design [2]. While the ICD-1 has evolved, it still follows the same path as the initial Project X proposal but with an increased beam current. A preliminary study of the slow beam extraction with the ICD-1 indicates intrinsic problems and lack of flexibility. The ICD-2 is motivated to address the deficiencies found in the ICD-1.

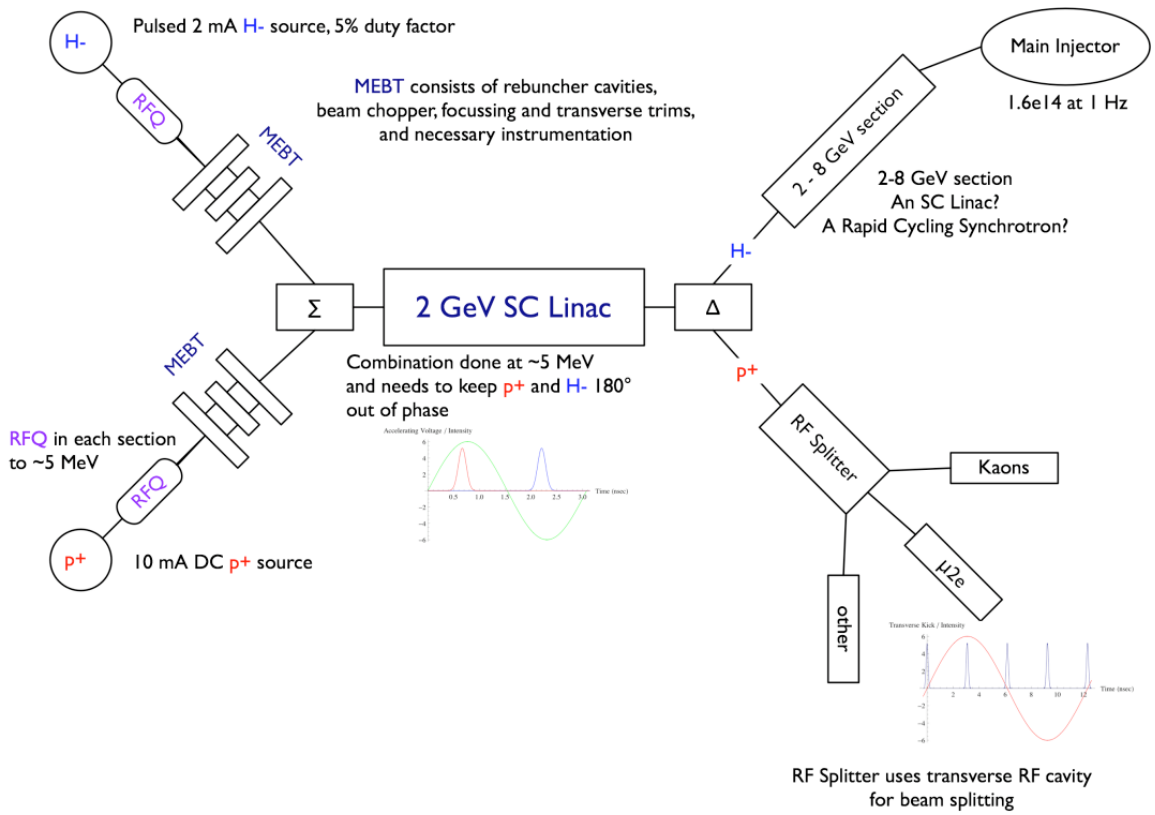

Figure 2: The schematic layout of the ACD concept

The main concept of the ICD-2 is to replace slow extracted beam at 8 GeV with the beam accelerated in a Continuous Wave (CW) linac operating with a nominal frequency of 325 MHz which could be implemented with 1300 MHz cavities. This concept has a number of notable advantages. First, the RF separation of the beam after acceleration allows simultaneous operation of several experiments (similar to the three hall operation at Jefferson Lab). The time structure and the intensity of each beam can be varied independently. Second, the beam quality of a CW linac is significantly better than for slowly extracted beams; in particular, the linac beam intensity does not have fluctuations inherent to slow extracted beam from a synchrotron. Third, the power of beam accelerated by a CW linac is set by high energy physics requirements (ability to use this power by experiment) rather than by technical or accelerator physics requirements.

Fourth, the bunch length in a linac (<10 ps rms) is much smaller than can be reasonably achieved in a ring which enables unprecedented Time-Of-Flight resolution that will be invaluable to next generation rare-decay experiments.

The energy of the linac is determined by the threshold of particle production. The linac energy of 1 GeV would be sufficient for muon production but the threshold of kaon production is slightly below 2 GeV. This sets the linac energy to 2 GeV. Note that this energy is below the threshold for anti-proton production which results in a reduced background for stopping muon experiments.

Energy, min/max, GeV	2/8
Repetition rate, Hz	10
Circumference, m (MI/6)	553.2
Tunes	18.44
Transition energy, GeV	13.36
Number of particles	2.67E13
Beam current at injection, (Amps)	2.2
Harmonic number	98
RF frequency, MHz	50.33 – 52.81
Maximum RF voltage, MV	1.2
95% n. emittance, mm mrad	25
Space charge tune shift at injection [1]	0.16
Norm. acceptance, mm mrad	40
Injection time for 1 mA, ms	4.3
Linac energy correction during injection	0.8%
RF bucket size, eV s	0.25
Number of RF cavities	10
Cavity shunt impedance, kΩ	100

Table 2. Main parameters of the synchrotron

Two MW Main Injector (MI) operation for the long-baseline neutrino program requires 8 GeV beam injection into the MI. Therefore an additional acceleration stage from 2 to 8 GeV is required in the ICD-2. This can be achieved with a synchrotron or a pulsed linac. Both choices require the linac beam current to be 1 mA or above. For the ICD-2 we choose a beam current to be 1 mA. This sets the total power of CW linac to 2 MW. Figure 2 presents a layout of the ICD-2 accelerator complex. To increase the reliability of the ion source we plan to have two ion sources: a pulsed one to supply H^- for strip injection and a continuous one to supply protons for the rare-decay physics program. These source beams are merged in the medium energy beam transport (MEBT) at 2-5 MeV. After the acceleration to 2 GeV the H^- and proton beams are split. The first one is directed to the MI, and the second one is split again and sent to three experimental halls.

[1] For a Gaussian beam at injection. The tune shift will be 3 times less for the KV distribution.

Presently, the ICD-2 studies are concentrating on a synchrotron for the 2-8 GeV acceleration stage. A pulsed linac is also possible; such a linac would be comparable to the ICD-1's 2-8 GeV portion. Table 2 presents the main parameters of the synchrotron. The circumference of the synchrotron should be kept sufficiently small to mitigate effects of the beam space charge and instabilities. We choose it to be 1/6 of MI circumference. This sets the repetition rate to be 10 Hz so that 6 injections could be delivered to the Recycler during a 0.8-s MI cycle at 60 GeV. The beam is stored in the Recycler and then it is transferred to the MI in a single transfer. Two out of eight injections sent to the Recycler in one MI cycle are available for a fast extraction 8-GeV program such as (g-2).

The use of a pulsed linac (2-8 GeV) instead of the synchrotron can be justified by co-development of ILC technology and a possible simplification of future upgrades for a neutrino factory or a muon collider. This pulsed linac should have a duty factor of 2-5%. The time structure of the linac can range from one 27-ms long pulse every 0.8-1.4 s (then a direct injection into the MI is possible) to a 2-ms pulse at 10-20 Hz with an injection (and accumulation) into the Recycler.

The accelerating gradient of the CW linac will be lower than that for the pulsed linac because of the larger cryogenic load. Roughly we can estimate the reduction from 25 MV/m (as in the ICD) to 18 MV/m. This results in lengthening of the CW linac relative to the corresponding part of the ICD-1 from 300 to 420 m.

Presently the future upgrades are determined by the needs of a neutrino factory and muon colliders. Both of these concepts require 2 to 4 MW beam power in the energy range of 8 to 20 GeV. In the case of a synchrotron the power increase can be achieved by increasing the synchrotron energy from 8 to 11 GeV, the repetition rate from 10 to 20 Hz, and by doubling the injected beam intensity. It will also require an increase of the CW linac current from 1 to 2 mA. Such an upgrade will be relatively inexpensive and will result in a beam power of about 2 MW at 11 GeV. In the case of a 2-8 GeV pulsed linac an upgrade will require a replacement of all linac RF sources. It will be more expensive than the described upgrade of the synchrotron but can deliver significantly higher power. The linac current increase from 1 to 25 mA would result in 4 MW power if pulse length and the repetition rate are not changed (2 ms and 10 Hz). The drawback of such an upgrade is that it requires the CW linac to be converted to a pulsed linac and a consequent termination of the corresponding 2 GeV physics program.

2.5 Beam power limitations of Slow Extracted Beam.

Estimates of beam power limits at 8.9 GeV/c per proton are provided for three different scenarios – using the present Booster with the antiproton source storage rings following the completion of Run II; using 8.9 GeV/c beam from Project X and the antiproton storage rings; and, using the Recycler fed from Project X.

Use of Debuncher via Booster

Plans are being developed to utilize the present antiproton storage rings for use in an 8.9 GeV/c fixed target program to support the initial phase Mu2e experiment and, perhaps, the muon g-2 measurement. The Mu2e experiment would receive slow spill from the Debuncher over a 667 ms time period, utilizing the beam provided from 3 pulses from the Booster. This gives an average beam power to the experiment of about 25 kW. A 2% beam loss at this level uniformly distributed about the Debuncher circumference presents a 1 W/m energy deposition in the ring, consistent with the present operation of the Fermilab Booster synchrotron. The Booster, however, loses much of its beam during multi-turn injection and adiabatic capture, and during the acceleration through its transition energy. Neither of these two effects will be present in the Debuncher or Accumulator rings. On the other hand, resonant extraction can present losses on the few-percent level, but as these are deposited at well-defined locations, they can be dealt with in a controlled fashion. Thus, it is not unreasonable to propose that with proper mitigation the beam power levels from the Accumulator/Debuncher can be increased from 25 kW.

If the Accumulator/Debuncher rings could accept and utilize every Booster pulse, at its present operational intensity of 4 Tp per pulse, and operating at a flat-out rate of 15 Hz, this would correspond to 60 Tp/s or 77 kW of beam power. So long as the losses are controlled with appropriate shielding at known loss points, this would be the expected rough power limit of the present system.

Use of Debuncher via Project X

An investigation has been performed in which the beam loss requirements, the existing Debuncher aperture, and a plausible bunch formation scenario were considered for generating Mu2e-quality beams utilizing a Project X 8 GeV linac, and the Recycler, Accumulator, and Debuncher rings.[Nag09-1] The total beam power provided to Mu2e in this scenario could be as high as 150 kW. Further investigations ([Nag09-2]) indicate that slow spill losses may limit the actual operation to roughly half of this value, consistent with the discussion of the previous paragraph, though more work is required to better understand this limit. Assuming that the limiting factor is the resonant extraction beam losses, similar limits may be set for other experiments such as Kaon physics programs that would presumably operate with a different beam structure. However, if localized losses can be dealt with satisfactorily, beam power at the 150 kW level would be a reasonable upper limit to expect under this scenario.

Use of Recycler via Project X

As the ICD-1 Project X linac can quickly fill the Main Injector via the Recycler, then in principle a slow spill program can be performed "under" the MI ramp during which time the Recycler is unused. In this scenario, the linac, pulsing at 2.5 Hz, delivers 20 mA beam to the Recycler (after transferring beam to the MI) over 1.25 ms for a total of 160 Tp. The total average beam power of the linac is 500 kW. Depending on the

duration of the MI ramp (0.7-1.4 sec), 200 – 350 kW is potentially available for fast or slow extraction from the Recycler. At 160 Tp per cycle the Recycler has substantial issues with space charge. To mitigate it the beam is "painted" transversely to the emittance of 20 pi mm-mr (norm, 95%) as well as longitudinally to 580 bunches at 53 MHz.

During the development of the ICD-1 a study was performed to look at the issue of slow spill, which concluded that the very large momentum spread generated during the injection and accumulation into the Recycler made it difficult to control the losses during extraction. [DJ08] High beam losses due to the dispersed phase space of the large momentum distribution made extraction from the Recycler unattractive and further consideration was dropped at that time. Since then, spurred by studies of extraction from the Debuncher associated with the Mu2e experiment, a new scenario for extraction of large momentum spread beams (beams with large tune spread, in general) has been suggested and is presently under study. [JJ09] However, the remaining issue for Recycler slow spill is the required transverse aperture. The required resonant phase-space step size of the extraction process, necessary for low loss operation, tends to limit the emittance of the beam to a value much smaller than the available Recycler aperture, which is 40 pi mm-mr. . Competing with this, the emittance is typically increased (or "painted") to combat space charge forces at high intensities. For example, an unbunched 400 Tp beam (corresponding to 400 kW over a 1.333 s cycle) in the Recycler with a transverse emittance of 20 pi mm-mr would have a space charge tune shift greater than 0.1, unacceptably large, especially for controlled resonant extraction.

In the above, unbunched beams – or, at least, many bunches of short extent – have been assumed. A bunching factor appropriate for Mu2e on the other hand would greatly increase the space charge tune shift, and so the intensities and beam power delivered to this type of experiment would be further limited, depending upon the design details of a Phase II Mu2e system.

From all of these considerations, beam power much greater than 150-200 kW from the Recycler using the ICD-1 linac appears impractical.

Use of a New Ring

Allowing for the possibility of a new ring, or set of rings, to be constructed for use in a slow spill program through Project X creates an opening for higher beam power to be contemplated at 8-10 GeV proton energies. As beam loss will inevitably be the limiting factor, a system with appropriate shielding, both for above-ground personnel protection as well as shielding of components in the tunnel, as well as radiation-hard components where required could allow for designs of rings of much higher power, the absolute limits of which would be hard to predict here. Low energy (8-16 GeV, kinetic) proton driver designs using the Fermilab Booster as an injector have been documented which would deliver beam power at the 0.5-1.2 MW range. [PD1,PD2] With the use of a Project X ICD-2 cw linac as a source, higher power beams at these levels should be possible through a new back-end synchrotron system with appropriate shielding precautions.

3. Rare Decay Physics with the ICD-2 Accelerator Complex

3.0 Modeling particle production from ICD-2 drive beam.

Since the time of the interim report there has been considerable effort by the Energy Deposition Department in the Accelerator Physics Center (APC) to model particle production in the challenging region of 1 GeV < T_p < 8 GeV (where T_p is the proton kinetic energy) on a variety of targets. These efforts are motivated by the broad interest in modeling particle production for the muon collider, mu2e, the $(g\text{-}2)_\mu$ initiative, rare kaon decay initiatives as well the basis for this task force study.

Pion production from both low-Z and high-Z targets have been modeled with fire-ball parameterizations of the HARP data as shown in figures 3 and 4

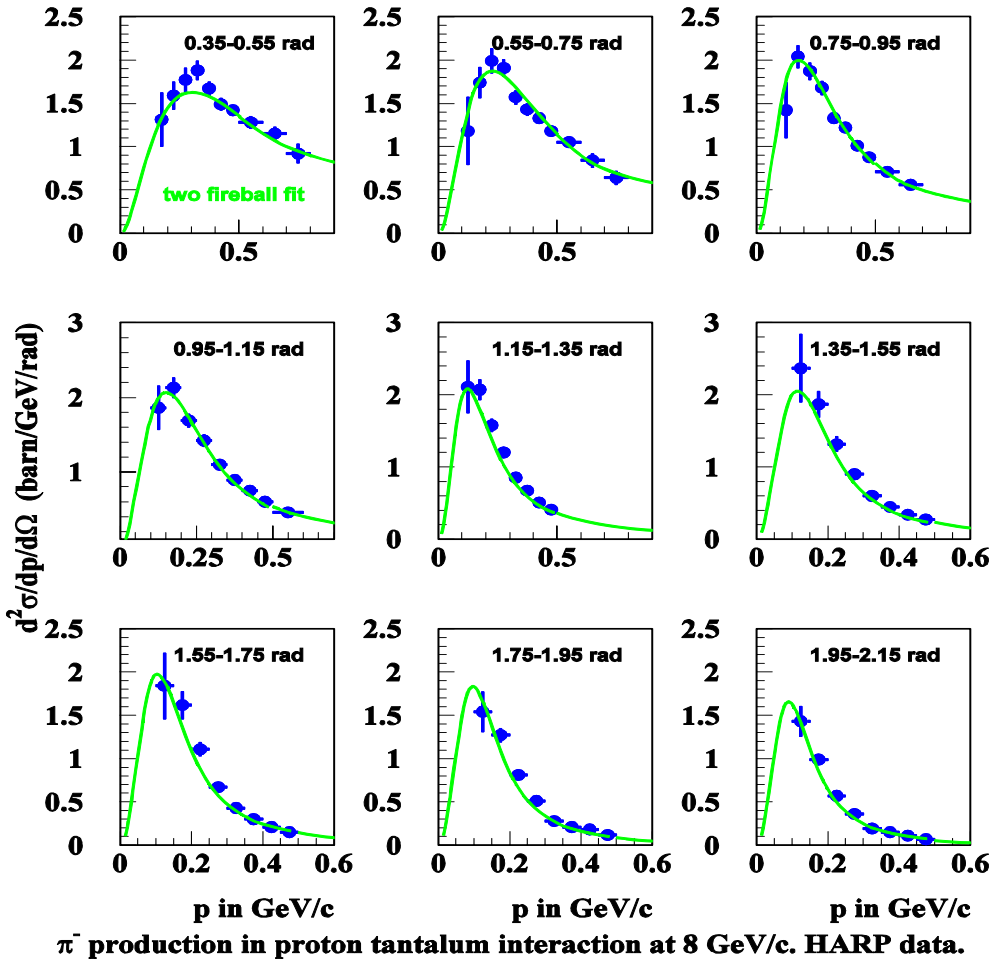

Figure 3 Modeling of the 8 GeV/c HARP data on tantalum.

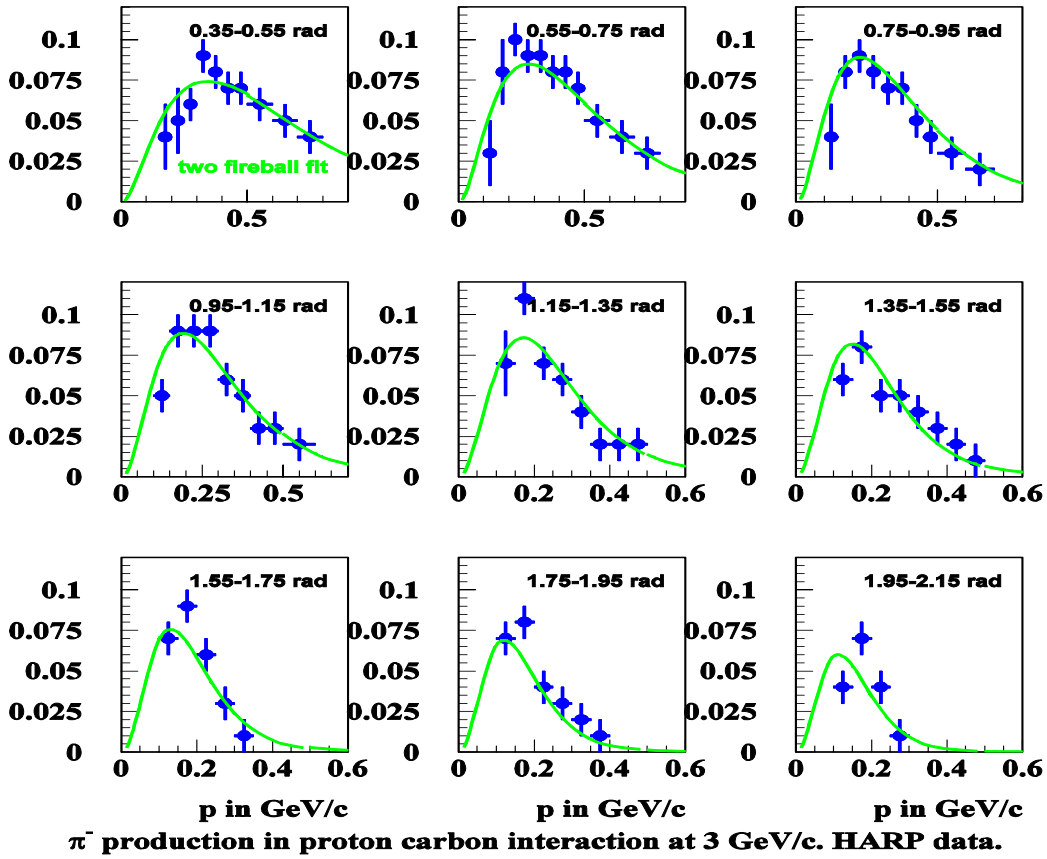

Figure 4 Modeling of the 3 GeV/c HARP data on carbon.

The fireball modeling supplements the LAQGSM (Los Alamos Quark-Gluon String Model) event generator in the MARS15 code for realistic simulation of various target/capture system configurations. The production of strange particles is simulated through explicit channels for $s^{1/2}$ <4.5 GeV which is a new module that has been added to LAQGSM:

In the LAQGSM code K, Λ, and Σ are produced by channels:

N+N→ K + Λ + N , π + N → K + Λ,
N+N→ K + Σ + N , π + N → K + Σ, for intermediate energies ($s^{1/2}$ <4.5 GeV),

At higher energies strangeness production is simulated with the existing LAQGSM modules:

B+B → K + Λ + X, M + B → K + Λ + X, B+B →K + AK + X,
B+B → K + Σ + X, M + B → K + Σ + X, M+M →K + AK + X

The energy dependence of cross sections in figures 5 and 6, and a precision benchmarking study is described in section 3.2.1.

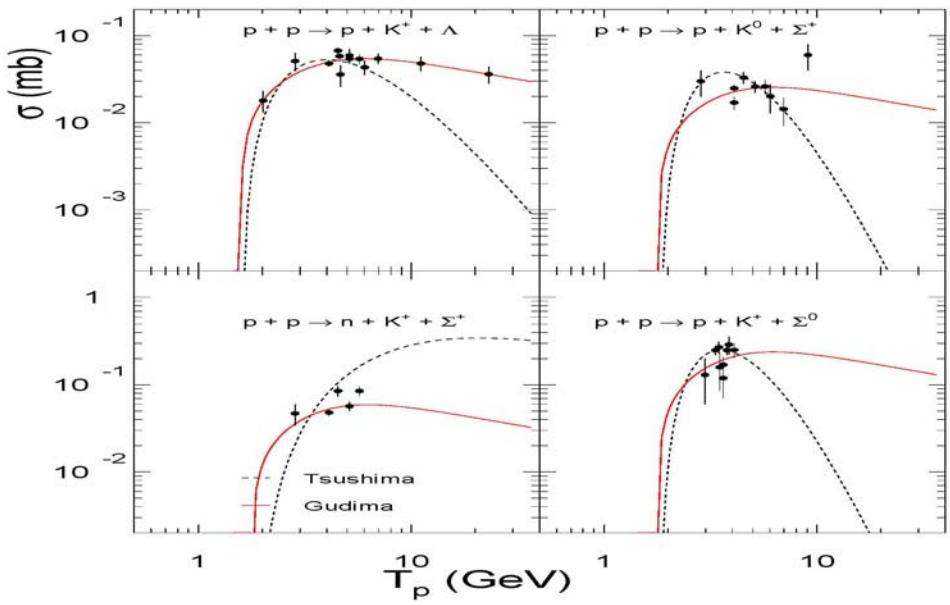

Figure 5: Strangeness production with protons through explicit channels now modeled with LAQGSM (red curve). Data points are from XXX.

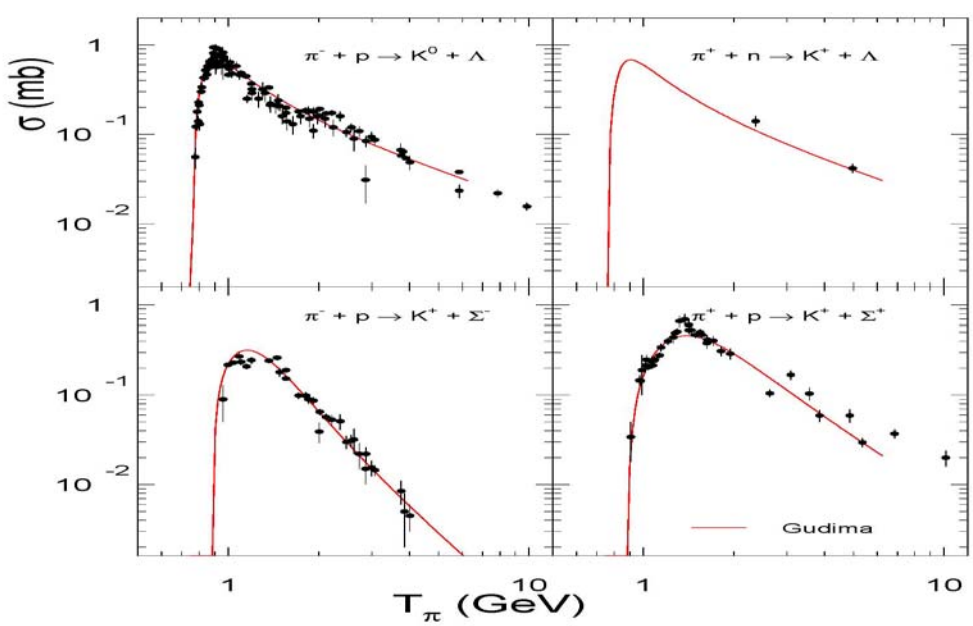

Figure 6: pion driven kaon production as modeled by LAQGSM (red curve). Data points are from XXX.

3.1 Next Generation Muon Experiments:

Muons stopped in the aluminum foils of the Mu2e experiment predominantly originate from pions with kinetic energy below 100 MeV. There are few experimental measurements for pion yields at these low energies. Thus the stopped muon yields for Mu2e rely on production models tuned to the measured π^- cross section for pions with larger kinetic energies and extrapolated to the region of interest. For an incident proton beam of 8 GeV the π^- yield at low kinetic energies varies by a factor of 2-3 depending on the choice of production model, e.g., MARS15 [4], LAQGSM [5] or FLUKA [6]. Benchmarking [7] confirms these uncertainties in production model predictions in this region.

From measurement of π^- yields from protons on Carbon and Lead/Tantalum at various incident proton energies we estimate that the *total* π^- yield for a 2 GeV (kinetic) proton beam is about a factor of 15 smaller per incident proton than for an 8 GeV beam. Using fits to FANCY data [8] data for 3 GeV/c protons on aluminum and 4 GeV/c protons on aluminum and lead, we can extrapolate the π^- yields to the lower kinetic energies. The fits reasonably reproduce HARP data [9] for 3 GeV/c protons on carbon, which extend down to pion kinetic energies of about 30 MeV. A prediction for the π^- yields for 8 GeV/c protons is obtained by normalizing the 4 GeV/c proton on lead fit from FANCY to HARP data for 8 GeV/c protons on lead for pions at large angles and kinetic energies above 100 MeV. After normalization, the FANCY fit reproduces the shape of the HARP data at large angles important for Mu2e. Based on these fits, the π^- yields for kinetic energies below 100 MeV scale roughly linearly with the proton kinetic energy independent of angle. Thick target effects can be important for low pion energies and have not yet been explicitly considered. We are planning to perform a systematic study of low energy pion yields for a 2-GeV proton beam, and hopefully to improve the production models used at Fermilab.

Despite the above uncertainties, there are several in-principle advantages in driving future stopping muon experiments with a 2 GeV CW linac. These are:

1) The CW linac proton beam can directly impinge on the production target with a very high duty factor which finesses the substantial challenge of extracting high power beam from a synchrotron.

2) Production model uncertainties in the low energy π^- yield from 2 GeV proton drive beam can be compensated with the large beam power reserve of the CW linac.

3) The extraordinary intra-pulse extinction required by stopping muon experiments (10^{-9}) is intrinsic to the CW linac accelerating structure. A secondary extinction channel may not be necessary.

4) Experimental backgrounds from kaons and anti-protons produced in the production target will be substantially reduced (eliminated in the case of anti-protons) with a 2 GeV drive beam.

3.1 Next Generation Muon Experiments

There are a variety of experiments using intense muon sources and offering the possibility of probing New Physics in ways complimentary to the collider program. These include searches for charged lepton flavor violating (CLFV) processes like $\mu^+ \rightarrow e^+e^-e^+$, $\mu^+ \rightarrow e^+\gamma$, and $\mu^- N \rightarrow e^- N$, other searches for lepton flavor number violating decays like muonium to anti-muonium conversion ($\mu^+e^- \rightarrow \mu^-e^+$), as well as precision measurements sensitive to New Physics effects like an improved determination of the $(g-2)_\mu$ or an improved limit on the EDM_μ. To fully elucidate the details of any New Physics discovered will require measurements of several of these properties. For example, while many New Physics scenarios which incorporate neutrino masses predict large enhancements to the rates of lepton flavor violating processes, the ratios of these rates is strongly model dependent. Thus a discovery in one experiment makes searches for other processes even more compelling since in combination these rates can help specify the underlying New Physics model responsible. Conversely, null results in one experiment don't necessarily rule-out a discovery in the other processes. In all cases the proposed sensitivities probe mass scales well beyond what will be accessible at the colliders. In general, searches for these LFV processes and related precision measurements offer a robust experimental program with significant sensitivity to New Physics effects in ways complimentary to the collider program.

The ICD-2 complex discussed in Section 2.4 will provide at least 1 mA of protons at 2.x GeV for a total beam power of 2MW for a suite of experiments in addition to the LBNE at DUSEL. The flexibility afforded by the RF splitter at the end of the CW linac allows for the possibility of exploiting these protons to simultaneously provide beam to multiple rare decay experiments. We summarize here the current status, beam requirements, and experimental limitations for measurements using muon beams. Where applicable we also discuss proposed endeavors at other facilities.

Most of the experiments we'll discuss require a source of stopped muons, and thus require an intense source of low energy (KE < 50 MeV) muons, which in turn originate from low energy pions (KE < 100 MeV). As discussed in the previous sub-section the yield of these low energy pions scales approximately linearly with the kinetic energy of the incident proton for the proton beam energies of interest. Thus the yield for a 2 GeV proton beam is expected to be about a factor of four smaller than an 8 GeV beam. This is fairly independent of production angle and is true for both π^+ and π^- production. This lower yield could be compensated for in a variety of ways. For example experiments designed for the ICD-2 complex could run longer and/or the 2 GeV linac could run at higher beam power and/or operate with a higher duty cycle relative to the 8 GeV option proposed in the ICD-1.

3.1.1 A Phase-II Mu2e experiment

The coherent conversion process, $\mu^- N \rightarrow e^- N$, is an example of a charged lepton flavor violating (CLFV) decay. In the SM this process can occur only through loop diagrams whose amplitudes are proportional to $(\Delta m^2_{ij} / M^2_w)^2$ where Δm^2_{ij} is the mass-squared difference between the ith and j^{th} neutrino mass eigenstates. Because the neutrino mass differences are so small relative to M_w the rates of CLFV decays in the SM are effectively zero (e.g. $<10^{-50}$ for both $\mu^+ \rightarrow e^+ \gamma$ and $\mu^- N \rightarrow e^- N$). Thus these CLFV processes offer a very theoretically clean place to search for New Physics effects. A wide array of New Physics (NP) models predict enormous enhancements to CLFV rates and to the $\mu^- N \rightarrow e^- N$ process in particular. Rates in the range of $10^{-15} - 10^{-17}$ are predicted, for example, in MSSM Super Symmetry, R-parity violating SuSy, leptoquark, extra dimension, new gauge boson, and extended higgs sector models [M.1]. An experiment with a sensitivity of 10^{-16} to the rate of $\mu^- N \rightarrow e^- N$ conversions would have an excellent discovery potential over a wide range of NP models.

The current best limit on the coherent conversion process is from the SINDRUM-II collaboration, which placed an upper limit of 4.3×10^{-12} at 90% CL for the coherent conversion of muons into electrons using a titanium stopping target [M.2]. In that paper they report one background event near the signal region (with energy 100.6 MeV), which they attribute to cosmic rays based on off-beam data. The collaboration added passive shielding to suppress cosmic ray background in an additional data-taking run, which aimed to improve the sensitivity by another order of magnitude. The result of this additional data taking was never published although a preliminary result was shown at a conference [M.3]. Events in the tail of the electron energy distribution were observed and it is speculated that these are either prompt backgrounds from radiative pion capture events, or cosmic ray induced events. The SINDRUM-II experiment used a DC beam and vetoed prompt events using information from a set of beam monitoring scintillators. This approach is limited by rate effects. The efficacy of the cosmic ray shielding employed is not described or discussed in any public documents that we are aware of.

The Phase-I Mu2e experiment plans to use 25 kW of 8 GeV protons to improve the sensitivity on the CLFV process $\mu^- N \rightarrow e^- N$ by four orders of magnitude to 5.7×10^{-17} at 90% CL. Assuming a technically driven schedule the Phase-I Mu2e experiment would be ready for data taking sometime in 2016. A Phase-II experiment has been discussed and assumes at least 150 kW of protons at 8 GeV in order to improve the sensitivity a further order of magnitude [M.4].

The Phase-I experiment proposes to use 8 GeV protons from the Booster and to establish the required 500 kHz of pulsed beam using the Recycler, Debuncher, and Accumulator rings [M.5]. The Mu2e duty factor during Nova operations may be relatively low (<50%). As discussed in Section 1.1 and Table 1 there are stringent requirements on the intra-pulse extinction for which there are conceptual designs for

meeting the Phase-I goal of 10^{-9}. For a Phase-II experiment an additional factor of 8 or so in beam power is envisioned, and an additional factor of 10 or more improvement in extinction would be necessary. It is doubtful that the Recycler, Debuncher, Accumulator complex could accommodate this much additional beam power. Space-charge effects in the Debuncher ring are likely to limit the beam power to less than 200 kW unless all effects leading to beam losses (such as space charge, tune jitter etc.) are understood and beam losses are collimated to an acceptable level. Fundamentally, the losses cannot be reduced to zero because the extraction process requires inserting a thin septum into the beam. The septum loss is typically not less than 2%. [M.6]. The additional improvement in the extinction is probably achievable as a straightforward extension of the Phase-I extinction channel.

For Phase-I Mu2e the optimal time between pulses is 1.7 μs, which is about twice the muon decay rate in aluminum $\tau_{\mu Al} = 0.86$ μs. It should be noted that the optimal pulse spacing might change depending on target material since the muon decay rate falls with increasing Z (e.g. $\tau_{\mu Ti} = 0.33$ μs). As discussed in the next paragraph, the stopping target choice for Phase-II Mu2e is unknown at this point, and thus the exact beam structure for Phase-II is difficult to specify.

The goals of a Phase-II Mu2e experiment depend on the results of the Phase-I experiment. If a signal is observed in the Phase-I experiment, then the Phase-II experiment will either aim to confirm the signal with a larger statistics data sample, or by changing the material in the stopping target. If no signal is observed in the Phase-I experiment, then the Phase-II experiment will aim to search for a signal with a sensitivity improved by about an order of magnitude. The signal is an isolated mono-energetic electron with an energy that depends on the nuclei in the stopping target. For an aluminum stopping target the electron energy for signal events, $\mu^- N(A,Z) \rightarrow e^- N(A,Z)$, is 104.96 MeV [M.7] The principal background challenges are the same for all these scenarios, although their relative importance may vary: the intrinsic muon Decay-in-Orbit (DIO) and Radiative muon Capture (RMC) backgrounds, the prompt background from Radiative pion Capture (RPC), and cosmic ray induced background events.

As the muons are stopped in the stopping target they are captured into a 1S orbit. For an aluminum target, about 40% of these muons in orbit will decay $\mu^- N(A,Z) \rightarrow e^- \nu\nu N(A,Z)$ [M.8]. The energy spectrum of the electrons has a sharp edge at about half the rest mass of the muon, but with a long tail from nuclear recoils extending to about 105 MeV. The spectrum falls as $\sim E^5$ in the region near 105 MeV so that the number of DIO electrons that satisfy the final selection criteria is a strong function of the spectrometer resolution of the experiment [M.9]. For the Phase-I experiment it is expected that the spectrometer resolution will be scattering dominated with the largest contributions coming from scatters in the stopping target downstream of the signal conversion event and from scatters in the proton/neutron absorbers situated just downstream of the stopping target. Since the DIO background scales with the number of stopped muons, its relative contribution can only be reduced by reducing the scattering contribution to the spectrometer resolution. For a Phase-II experiment this could be accomplished by shrinking the stopping target and/or by shrinking or removing the proton/neutron

absorbers. In order to maintain a reasonable ratio of stopped-muons per POT this might necessitate a smaller momentum spread in the beam muons, peaked at lower kinetic energies (~40 MeV) in order to compensate for a smaller stopping target. Removing or otherwise mitigating the rate induced by neutrons and protons knocked-out as the muon pulse arrives at the stopping target would allow a reduction in or the removal of the proton/neutron absorbers.

The other 60% of the stopped muons will be captured on the nucleus [M.10]. About 10^{-5} of these nuclear captures will be radiative and yield a photon with an energy above 57 MeV. Occasionally the photon will be energetic enough (>103 MeV) and will asymmetrically pair produce in detector material to yield a signal-like electron [M.4]. This RMC background also scales with the number of stopped muons and thus can only be mitigated by improving the experiment design. In this instance, as with the DIO background, a reduction in the target material will reduce this background contribution.

In analogy to RMC, pions which reach the stopping target can be captured on the nucleus and will, about 2% of the time, emit a photon [M.11] which can asymmetrically pair produce in detector material to yield a signal-like electron. The pion capture process is effectively instantaneous so that this is an example of a "prompt background" since it will appear in time with the arrival of the muon beam at the stopping target. By using a pulsed beam this background can be suppressed by defining a signal window that is several 100 ns delayed relative to the beam arrival at the stopping target. Then, only pions created by out-of-time protons impinging on the production target can contribute to the final background. The extinction requirement for the Phase-I experiment is defined to keep the RPC background small (<0.1 event). For the Phase-II experiment the number of late pions arriving at the stopping target will have to be reduced in proportion with the increase in beam power. This can be achieved by improving the extinction or by reducing the fraction of pions at the production target which survive to reach the stopping target by modifying or changing the transport beam line.

The cosmic ray background is continuously illuminating the experiment. Using a pulsed beam structure helps reduce the sensitivity of the experiment to cosmic rays. Passive shielding is employed to further reduce the rate of cosmic rays reaching the Mu2e detector. An active shield is employed to identify and veto potential cosmic ray background events. This background scales with running time. Assuming the run time of a Phase-II experiment is comparable to the Phase-I experiment, then the Phase-I cosmic ray veto system should suffice for the Phase-II experiment as well.

For a Phase-II experiment the increased beam power would increase the instantaneous rates at which the detector must reliably operate. Simulations indicate that this is probably feasible, but this has yet to be empirically demonstrated. If necessary, the rates of a Phase-II experiment could be controlled by improving the duty cycle, improving the yield of stopped-muons per POT, or extending the experiment run time relative to the Phase-I program.

The COMET experiment at J-PARC [M.12] is another muon conversion experiment with a design sensitivity comparable to the Phase-I Mu2e experiment. The COMET and Mu2e beam lines are similar since both inherited from the MECO portion of the RSVP proposal at BNL [M.13]. The main difference is that the transport solenoid for the Mu2e proposal is S-shaped while for the COMET proposal it is C-shaped. A comparison of the relative merits of each design is being made by both collaborations. The COMET and Phase-I Mu2e detector designs are optimized differently, with Mu2e proposing to use a cylindrical spectrometer and COMET proposing to use a C-shaped spectrometer. Nevertheless, the dominant background contributions are the same for the two proposals. COMET cannot be run simultaneously with the J-PARC neutrino program and dedicated beam time has yet to be scheduled. The COMET detector would be ready for data-taking sometime in 2016 assuming a technically driven schedule. J-PARC also has a conceptual design for an experiment that would improve the sensitivity of COMET by an order of magnitude and would compete with a Phase-II Mu2e experiment. The PRIME experiment would operate at the PRISM muon facility.

3.1.2 The Prism concept

The discussion of 3.1.1 for a Phase-II Mu2e experiment assumes that the muon beam line is conceptually the same as that used for Phase-I and employs a graded magnetic field in the region of the production target to capture mostly backwards going low energy pions and transport them to the stopping targets via a long curved decay solenoid. Under this assumption, to keep the prompt backgrounds under control, a Phase-II beam line will have to improve the extinction in proportion to the increase in beam power. There are a few ideas about alternative production and transport beam lines that may prove better for a Phase-II experiment. For example, it may be possible to capture the forward going pions at the production target and then employ a system of helical cooling channels and degraders to reduce the momentum spread and improve the π/μ ratio in the beam [M.15].

The most mature alternative idea is the PRISM proposal at J-PARC, which would capture, store, and cool muons using fixed field alternating gradient (FFAG) magnets. The PRISM storage ring requires a source of pulsed muons as input. The muons are captured and phase rotated in the storage ring to reduce the momentum spread from 30% to 3%. This reduction in the momentum spread of the extracted muons would allow a reduction in the thickness of the stopping target and thus a reduction in the intrinsic DIO background. Pion backgrounds will also be reduced by storing the beam in the ring for an extended period of time to allow the pions to decay away. In the PRISM proposal the pion survival rate is estimated to be 10^{-20}. Additional inter-pulse beam extinction will come from the kicker magnets at injection and extraction from the FFAG ring. A phased R&D program has begun at J-PARC to address the issues related to this concept.

3.1.3 A $\mu^+ \rightarrow e^+\gamma$ experiment

Another CLFV process is the decay $\mu^+ \rightarrow e^+\gamma$, which can occur at rates as large as 10^{-13} in some models. In general this process is principally sensitive to models in which the

New Physics contributes via loops (e.g. SuSy). The current best sensitivity was achieved by the MEGA collaboration which places an upper limit on the $\mu^+ \rightarrow e^+\gamma$ branching fraction of 1.2 x 10^{-11} at 90% CL [M.16]. The MEG collaboration recently released preliminary results from their first physics run [M.17]. The MEG experiment aims to achieve a sensitivity of 10^{-13} sometime in the next few years and may reach the 10^{-14} level with some upgrades and an extended data-taking run beyond that. The μ^+ are stopped in a thin target so that signal events yield a back-to-back positron and photon, coincident in time, each with an energy of half the muon mass. The background has contributions from radiative muon decay, $\mu^+ \rightarrow e^+\gamma\nu\nu$, when the neutrinos carry away very little momentum, and from the more dominant accidental overlap of a positron from standard muon decays with a stray photon. Since the accidental backgrounds are a strong function of detector rates, a continuous muon beam is probably an advantage. The accidental background is a function of the timing, energy, and angular resolutions of the detector. The MEG experiment aims to achieve a positron energy resolution of 1% using a low mass spectrometer, a photon energy resolution of 4.5% using a liquid xenon calorimeter, an angular resolution between the positron and photon of 19 mrad, and a timing resolution of 0.15 ns. Unless these resolutions can be significantly improved, it is unlikely that the MEG sensitivity can be readily improved upon.

3.1.4 A $\mu^+ \rightarrow e^+e^-e^+$ experiment

The CLFV process $\mu^+ \rightarrow e^+e^-e^+$ is sensitive to the same New Physics diagrams via photonic penguins as the $\mu^+ \rightarrow e^+\gamma$ process. However, in addition to the photonic penguin, the $\mu^+ \rightarrow e^+e^-e^+$ process is also sensitive to Z penguin and higgs penguin diagrams. In most models the photonic penguins dominate, but since the final state in the $\mu^+ \rightarrow e^+e^-e^+$ decay consists of three charged particles, it offers additional experimental handles with which to suppress the dominant accidental backgrounds. The current best sensitivity was achieved by the SINDRUM-I experiment which placed an upper limit on the $\mu^+ \rightarrow e^+e^-e^+$ braching fraction of 1×10^{-12} at 90% CL [M.18]. The μ^+ are stopped in a thin target so that signal events are characterized by an electron and two positrons originating from the same vertex position within the stopping target, coincident in time, and with a total momentum of zero and a total energy equaling the mass of the muon. Since this is a three body decay the momentum of the positrons extends to low values and overlaps with the spectra from standard muon decays. This then presents the principal experimental challenge – building a spectrometer with excellent momentum and timing resolution, good vertexing capabilities, and capable of withstanding the high rates induced from the copious $\mu^+ \rightarrow e^+\nu\nu$, decays. Like the $\mu^+ \rightarrow e^+\gamma$ experiments, since accidental backgrounds are limiting, a continuous beam is beneficial because it keeps the instantaneous rates lower than a pulsed beam. There has been some informal discussions of mounting a new $\mu^+ \rightarrow e^+e^-e^+$ experiment at PSI with a sensitivity goal of 10^{-16} [M.19].

3.1.5 A $\mu^+e^- \rightarrow \mu^-e^+$ conversion experiment

The spontaneous conversion of a muonium atom (M = a μ^+e^- bound state) into an anti-muonium atom (Mbar = a μ^-e^+ bound state) violates lepton flavor number by two

units while conserving the total lepton number. It would be an analogy in the lepton sector to the well known K^0 and B^0 oscillations in the quark sector. Muonium-Anti-muonium conversion appears naturally in many New Physics theories. The interaction could be mediated by a doubly charged Higgs boson, Majorana neutrinos, a neutral scalar, a supersymmetric τ-sneutrino , or a doubly charged bileptonic gauge boson [M.20][M.21]. Typically, the muonium conversion results are expressed in term of $G_{M\text{-}Mbar}$, which represents the coupling constant for the 4-point interaction. There is a long history of searches for muonium oscillations starting in the 1960s with the pioneering work of Vernon Hughes. The latest results of such searches are from 1999 from the MACS collaboration at PSI [M.22]. The MACS spectrometer was designed to identify in coincidence the electron and the positron released in the anti-muonium decay. An energetic electron arises from the decay $\mu^- \rightarrow e^- \nu\nu$ with a characteristic Michel energy distribution extending to 53 MeV, and a positron appears with an average kinetic energy of 13.5 eV corresponding to its momentum distribution in the atomic 1s state of anti-muonium. The electron momentum was measured using multiwire proportional chambers with a resolution limited by the 2mm wire spacing. The atomic shell e^+ was electrostatically accelerated and detected on a microchannel plate detector. The PSI μ^+ beam provided a central momentum of 26 MeV/c and rates up to $8\text{x}10^6$ μ^+/s. The data taking lasted 6 months and a total of $5.6\text{x}10^{10}$ M atoms were investigated for Mbar decays. The resulting upper limit on $G_{M\text{-}Mbar}$ was $3.0\text{x}10^{-3}G_F$ at 90% CL. The background in MACS was dominated by accidental coincidences of energetic electrons produced by Bhabha scattering of positrons from M decays. Additional backgrounds can come from the rare muon decay $\mu^+ \rightarrow e^+e^-e^+\nu\nu$ with branching ratio $3.4\text{x}10^{-5}$ in which the electron is energetic and one of the positrons goes undetected.

A future intense pulsed muon beam could be an ideal place to search for M-Mbar conversion. In contrast to other lepton flavor number violating muon decays, the M-Mbar conversion through its nature as particle-antiparticle oscillation has a time evolution in which the probability for finding a system formed as muonium decaying as anti-muonium increases quadratically in time. This gives the signal an advantage, which grows in time over exponentially decaying background. The backgrounds can also be suppressed using a more precise tracking system for better reconstructing the decay vertex and the electron momentum. The rates required to significantly improve the sensitivity of this measurement are small compared to those required by the CLFV decays discussed in the previous sub-sections.

To our knowledge there is no planned experiment in the near future to search for muonium oscillations but there are discussions about hosting such experiment at the J-PARC facility.

3.1.6 A Project-X era $(g\text{-}2)_\mu$ experiment

A precision measurement of the anomalous magnetic moment of the muon, $a_\mu = (g\text{-}2)_\mu/2$, can be compared to precise SM calculations. Deviations between the observed value and the SM prediction can be used to constrain New Physics contributions, which contribute at the loop level. For example, in the context of SuSy, a precision a_μ can help

constrain tanβ , the ratio of the higg's vacuum expectation values, and determine the sign of μ, the gaugino mixing parameter.

The most precise determination of a_μ is from the Muon g-2 experiment at Brookhaven with a total relative uncertainty of 0.54 ppm, dominated by statistical uncertainties [M.23]. The precision of this measurement requires that the theoretical calculation include the effects of higher order quantum loop corrections. The SM prediction is known with an uncertainty comparable to the experimental uncertainty. The theoretical uncertainty is dominated by contributions from hadronic vacuum polarization (HVP) uncertainties [M.24]. The HVP component of the prediction is, in turn, limited by the uncertainties and consistency of experimental measurements using low energy e^+e^- data and τ lepton decay data as well as uncertainties arising from non-perturbative QCD calculations. At present the discrepancy between the measured and SM predicted a_μ is at about the 3.5σ level [M.24].

There is a proposal to improve the experimental precision on a_μ by a factor of four, down to 0.14 ppm, by re-locating the BNL storage ring to Fermilab and using the 8 GeV proton source once the Tevatron program is completed [M.25]. This experiment could begin taking data as early as FY2015 and would collect the necessary statistics in a two year run. It is anticipated that some modest improvements to the theory uncertainty will also occur on this same time scale, mostly due to improvements in the experimental inputs necessary for the HVP calculation.

If the experiment proposed in Ref. [M.25] has not been performed by the time the ICD-2 is experiment-ready, then the value of performing such an experiment should be revisited in the context of the future experimental and theoretical landscape. Discoveries from Phase-I Mu2e or at the colliders might make the resolution of the a_μ discrepancy even more compelling since it can help untangle which New Physics models are consistent with all the data. The intensity of the ICD-2 source would not be necessary to achieve the 0.14 ppm precision using a μ^+ beam. However, it could prove advantageous in repeating the measurement using a μ^- beam since the π^- production cross section is suppressed by a factor of three relative to the π^+ production cross section assuming an 8 GeV proton beam. Assuming CPT invariance, the comparison of the a_μ values determined from the μ^+ and μ^- beams offers a cross-check of many systematic uncertainties associated with the understanding of the magnetic fields since the polarities of all the dipoles, kickers, and focusing magnets need to be reversed. The comparison is also a test of Lorentz invariance. The proposal in Ref. [M.25] only uses a μ^+ beam, so that in the case that this experiment has been performed, it may still be worth considering a μ^- run exploiting the increased beam intensities at the ICD-2. It is anticipated that in this instance the theoretical uncertainty will be about a factor of three larger than the projected 0.14 ppm experimental uncertainty. In this scenario the μ^- run wouldn't significantly improve the precision on the experiment-theory comparison, but would primarily be useful as a cross check of the experimental number. Another possibility would be to use a μ^+ beam, but exploit the increased intensity of Project-X to select only a very narrow momentum band for acceptance into the storage ring. By storing the beam

within a very narrow emmittance it is expected a further reduction in the experimental systematics may be achieved. If a cross-check is deemed important, then it may be worth considering a methodology that's completely different than the traditional storage ring using the "magic momentum". A recent idea uses a muonium source, which is laser ionized to produce a low energy muon beam with a momentum spread of only $\Delta p/p < 10^{-5}$ [M.26]. This ultra-cold muon beam could then be stored in a "ultra-precision" magnetic field so that no electric field is necessary and the "magic momentum" term drops out of the expression for the spin precession frequency. While it's still unclear whether or not such a methodology is viable, it would offer a measure of a_μ with a completely different set of systematic uncertainties. Since it requires a muonium source, there may be an opportunity to share resources and infrastructure with a muonium conversion experiment. Under this scenario a low energy pulsed muon beam would be required.

It should be noted that the storage ring options discussed above require muons of 3 GeV so that the 2 GeV protons from the CW linac of the ICD-2 proposal are not energetic enough. Instead, for the ICD-2 proposal, a $(g\text{-}2)_\mu$ experiment would have to run in parallel with the neutrino program off the 8 GeV ring. This possibility should be kept in mind when specifying the design criteria of the 8 GeV portion of Project-X (for the ICD-1 a pulsed linac brings the protons to 8 GeV, while in the ICD-2 a synchrotron is used to accomplish the same thing). If instead the idea of using a laser ionized muonium source is pursued, then a 2 GeV proton source would work well.

3.1.7 A EDM_μ experiment

Any measurement of CLFV processes would imply the existence of a 3 x 3 mixing matrix similar to the CKM matrix for quarks and the PMNS matrix for neutrinos. One can easily envision a large experimental program focused on determining the various magnitudes and phases of the elements of this matrix in an attempt to pin down the symmetry breaking mechanisms associated with lepton flavor generation. As mentioned elsewhere in the text, $\mu \rightarrow e$ conversion in the field of a nucleus and decays such as $\mu \rightarrow e\gamma$, $\tau \rightarrow \mu\gamma$ and $\tau \rightarrow e\gamma$ will pin down the magnitudes of the off diagonal terms while g-2 measurements of all three leptons can pin down the diagonal elements. But as is well known, a 3 x 3 mixing matrix allows for the presence of a CP violating phase. Probing this phase is the topic of discussion here.

In Dirac's original work incorporating relativity into quantum mechanics [M.27], he pointed out that the promotion of the electron wave function into a spinor lead to extra terms in the coupling of an electron to an external electromagnetic field. The coupling to the magnetic field contained the correct g-factor g = 2 and was seen as a great success of the Dirac theory. The coupling to the electric field violated both parity and time reversal symmetry and would appear equivalent to a permanent electric dipole moment (EDM) for the electron. However, since this coupling was pure imaginary, it was dismissed as unphysical. Now, operators with real and imaginary terms leading to CP violating observables are present both in the standard model and essentially all its extensions [M.1]. It is then natural to use EDMs to probe for the presence of CP violating phases in the charged lepton mixing matrix. For example, EDMs have been probed to the level of

10^{-27} e-cm for electrons [M.28] and 10^{-28} e-cm for Mercury atoms [M.29] placing stringent bounds on 1st generation CP violating effects in the charged lepton mixing matrix.

The second generation can be probed with muon EDM measurements that to date have been performed parasitically in muon g-2 experiments [M.23][M.30]. In modern muon g-2 experiments, relativistic, polarized muons circulate in a storage ring with a uniform vertical magnetic field. In the muon rest frame, the muon sees a large motional electric field in the horizontal plane. A permanent EDM would feel a torque from this electric field which would tilt the precess leading to an up-down asymmetry in the flight direction of the muon's positron daughters. Recently, the Brookhaven g-2 experiment has used this technique to limit the muon EDM to less than $d_\mu < 1.9 \times 10^{-19}$ e-cm at the 95% CL and the new g-2 experiment at Fermilab plans to push this down another two orders of magnitude [M.25].

One can get an idea of the interesting regions of a muon EDM limit from the g-2 anomalous magnetic moment measurement a_μ. The a_μ measurement differs form expectation by approximately 3×10^{-9}. If this difference is due to a new operator, O^{NP} we could parameterize its effects on a_μ as $\mathrm{Re}(O)\cos\phi$ and its effects on an EDM as $\mathrm{Im}(O)\sin\phi$ where ϕ is a CP violating phase. The corresponding EDM is then related to the new physics contribution to a_μ by

$$d_\mu^{NP} = 3\times 10^{-22}\left(\frac{a_\mu^{NP}}{3\times 10^{-9}}\right)\tan\phi$$

in units of e-cm [M.31]. From this we see that it is clearly desirable to have a muon EDM experiment that can probe for an EDM well below the 10^{-22} level. A concept for an experiment to probe the muon EDM at the 10^{-24} has been put together by a collaboration largely overlapping with the Brookhaven and Fermilab g-2 collaborations [M.32].

Since the EDM measurements are performed parasitically to the g-2 measurements, they are far from optimized. In particular, the magnetic spin precession has two detrimental effects on the EDM measurement. First, the EDM effect is maximized when the spin is aligned with the electric field, not the magnetic field as is the case for the g-2 experiments. Secondly, the large magnetic spin precession motion can easily couple into the EDM measurement by causing apparent up down asymmetries and leading to other systematic effects. These effects can be removed by effectively turning off the magnetic precession frequency.

The magnetic precession frequency is given by

$$\vec{\omega}_a = \frac{e}{m}\left[a_\mu \vec{B} - \left(a_\mu - \left(\frac{1}{\gamma^2 - 1}\right)\right)\frac{\vec{\beta}\times\vec{E}}{c}\right]$$

The well known trick of the g-2 experiments is to run with 3.1 GeV muons ($\gamma = 29.3$ for $a_\mu \sim \alpha/2\pi$ to order α) which causes the second term to drop out of ω_a. However, with the appropriate momentum choice and the introduction of radial electric fields, the entire magnetic precession frequency can be removed and thus the only remaining non-orbital motion would be attributed to a muon EDM.

The experimental apparatus would consist of a muon storage ring of around 10 meter radius circulating muons at about 0.5 GeV in a 0.24 T field. A radial electric field of ~100 kV would be applied using concentric plates separated by ~10 cm. For polarized muons entering the ring, the spin is in the direction of the muon. As the muons circulate through the ring, the torque on the EDM from the motional field will cause the spin to slowly tilt out of the horizontal plane. The tilt angle increases with time allowing the effect to accumulate with longer storage time. The effect is a time dependent increase or decrease in positrons seen in detectors placed above or below the storage region.

Several sources of systematic uncertainties have been considered and many solutions have been incorporated into the experimental design. Assuming running at the AGS, the expected sensitivity was 10^{-24} e-cm. In most cases, knowledge and ability to produce the g-2 measurement feeds directly into this measurement making this a natural follow up for the Fermilab g-2 measurement. The lower muon momentum is also well matched to the ICD-2 2 GeV proton beam.

3.1.8 Other possibilities

There are a variety of other experiments which probe topics outside of particle physics such as muon catalyzed fusion experiments, precision determinations of the muon decay lifetimes and spectra from muon capture on various nuclei, precision measurements of muonium hyperfine structure, etc. Such experiments might benefit from the intense muon beams that would be made available by the ICD-2. Further progress on this front would require engaging the relevant scientific communities in a discussion of the opportunities the ICD-2 offers.

3.2 Next Generation Kaon Experiments:

The total pp cross section as a function of beam energy is shown in Figure 7 (PDG). As shown previously in figure 5, the proton kinetic beam energy (T_p) threshold for producing kaons is 1.7 GeV (on protons) and the kaon yield fraction grows with the increasing number of exclusive production channels that open and saturate around T_p of 5 GeV. Above 5 GeV the rate of useful kaons in a secondary beam is typically proportional to proton beam power, and hence many previous experiments were designed around relatively high energy proton drive beams extracted from synchrotrons. As noted in section 2.2 however the resonant extraction process does not scale well to next generation kaon experiments that will require in excess of 100 kW of beam on target. Reaching beyond these extraction limitations is a principle motivation for considering the ICD-2 conceptual design. Several previous kaon factory studies, notably the CERN 2001 study [Ref], concluded that the optimum drive proton beam energy is greater than

20 GeV for next generation experiments. This conclusion was based on the definition of the useable kaon momentum spectrum to be 2-20 GeV/c, and hence this conclusion depends strongly on the definition of useful kaons. The frontier today however in measuring the sought after $K^+ \rightarrow \pi^+ \nu\nu$ process for example was delivered by the stopped K^+ experiment at Brookhaven Natioal Laboratory (BNL) [Ref] driven by kaons of momenta less than 1 GeV/c. Hence it is worth considering next generation kaon experiments fueled by low energy kaons which can be copiously produced with ICD-2.

The threshold production channels for kaons in pp interactions is illustrated in Figure 8 which is based on data from the COSY (Cooler-Synchrotron) facility in Germany [Ref XX].

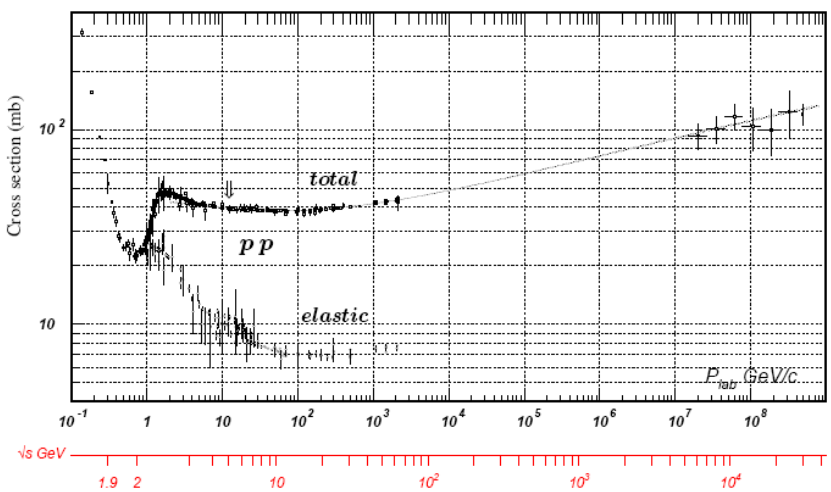

Figure 7: pp total cross section vs p beam momentum.

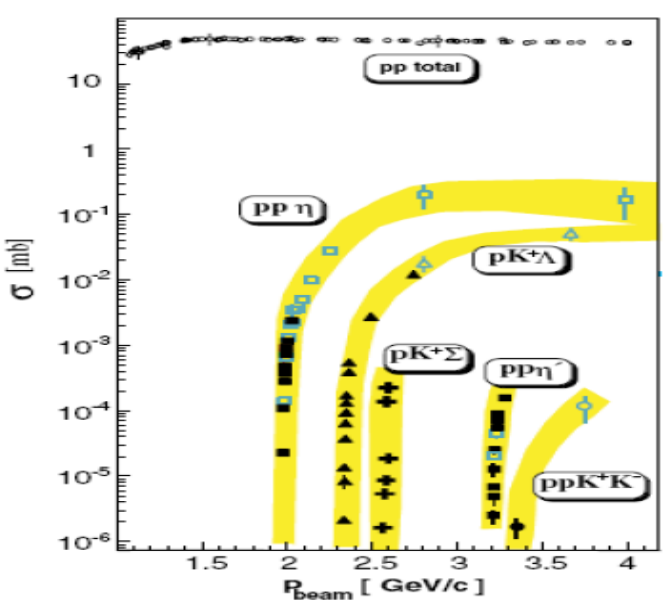

Figure 8. (Strangeness production thresholds of exclusive channels measured at COSY)

The COSY facility has an active research program that has produced high quality measurements of kaon production near threshold on a variety of target materials. As described in section 3.0 the Energy Deposition Department in the Fermilab Accelerator Physics Center has developed a new comprehensive simulation module in the LAQGSM/MARS framework for particle production in the challenging T_p region of 1-4 GeV. Kaon production in this module is treated as a sum of well measured exclusive channels with little tuning. The simulations have been benchmarked with COSY data, and one such benchmark is shown in figure 9 which is an absolute prediction of forward K^+ production yield on carbon and is in good agreement with COSY data.

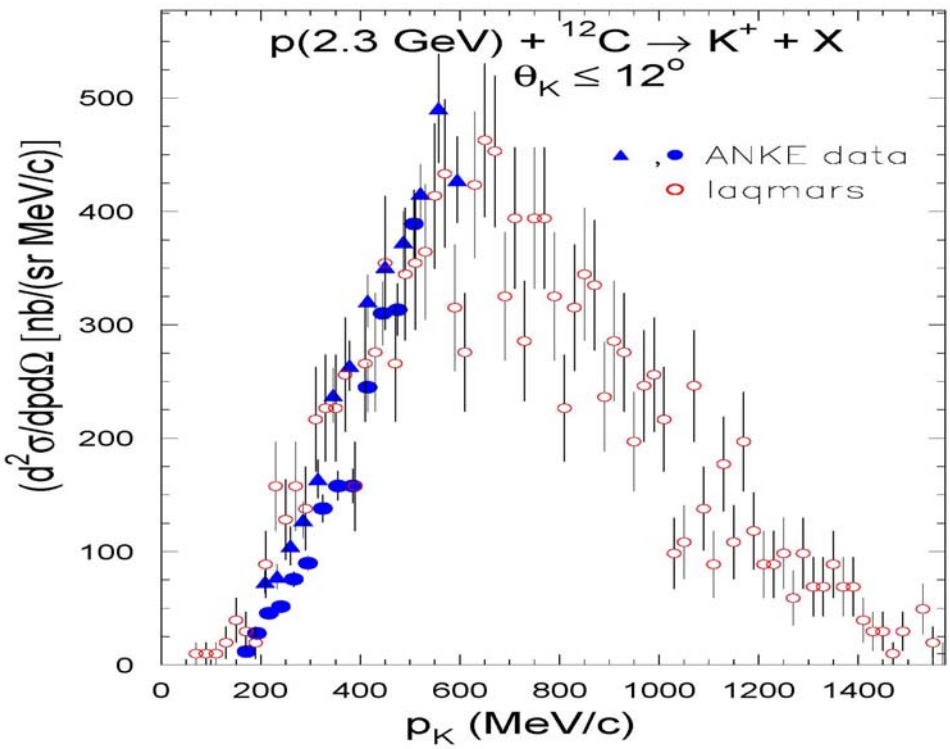

Figure 9. K^+ momentum spectrum from 2.3 GeV protons (kinetic) on a thin carbon target simulated with LAQGSM/MARS [5]. The simulated rate is absolutely normalized, and models the measured (ANKE) momentum spectrum and rate quite well.

Past kaon experiments driven with relatively high energy proton beams often optimized kaon yields with high-Z thick targets where secondary interactions can boost the kaon yield by up to 30%. Next generation experiments driven with high-power low-energy ICD-2 beams are better served with low-Z targets, such as carbon which has high kaon transparency, low spallation neutron yield, and excellent thermal properties for beam power management. MARS15 modeling of a realistic thick carbon target confirms that kaon beams and the associated backgrounds propagated to a detector closely resemble the scaled yield of the thin target studies presented in figures 10,11, and 12. .

The Kaon yield per interaction as a function of T_p on carbon for a variety of production angles and momenta are shown in figures 10 and 11. It is clear from figures 10 and 11 that the enormous ICD-2 beam current of 1 mA (6×10^{15} p/second) motivates consideration of high sensitivity kaon decay experiments with ICD-2 drive beams.

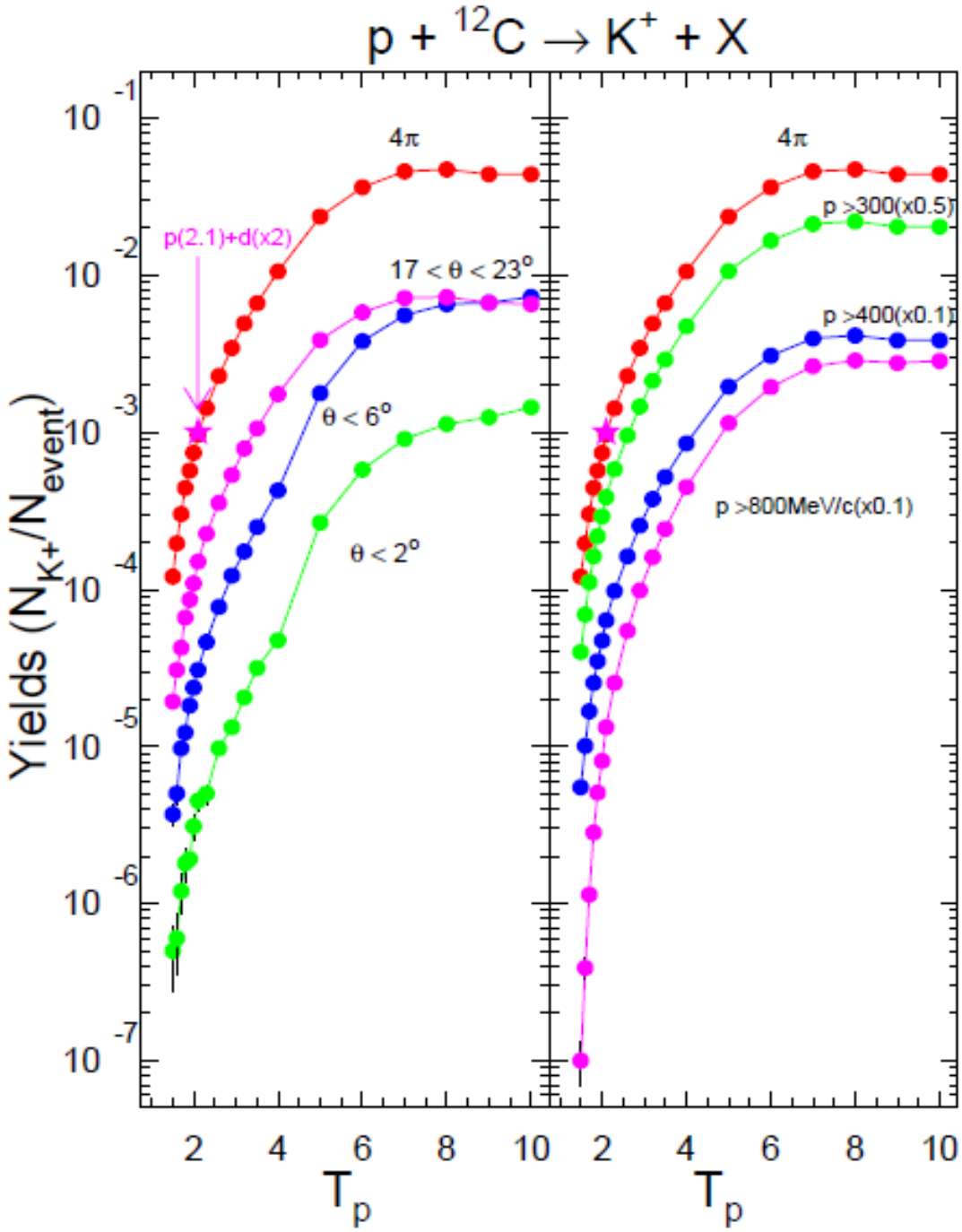

Figure 10. LAQGSM K^+ yield as a function of T_p (GeV), kaon momentum and angles.

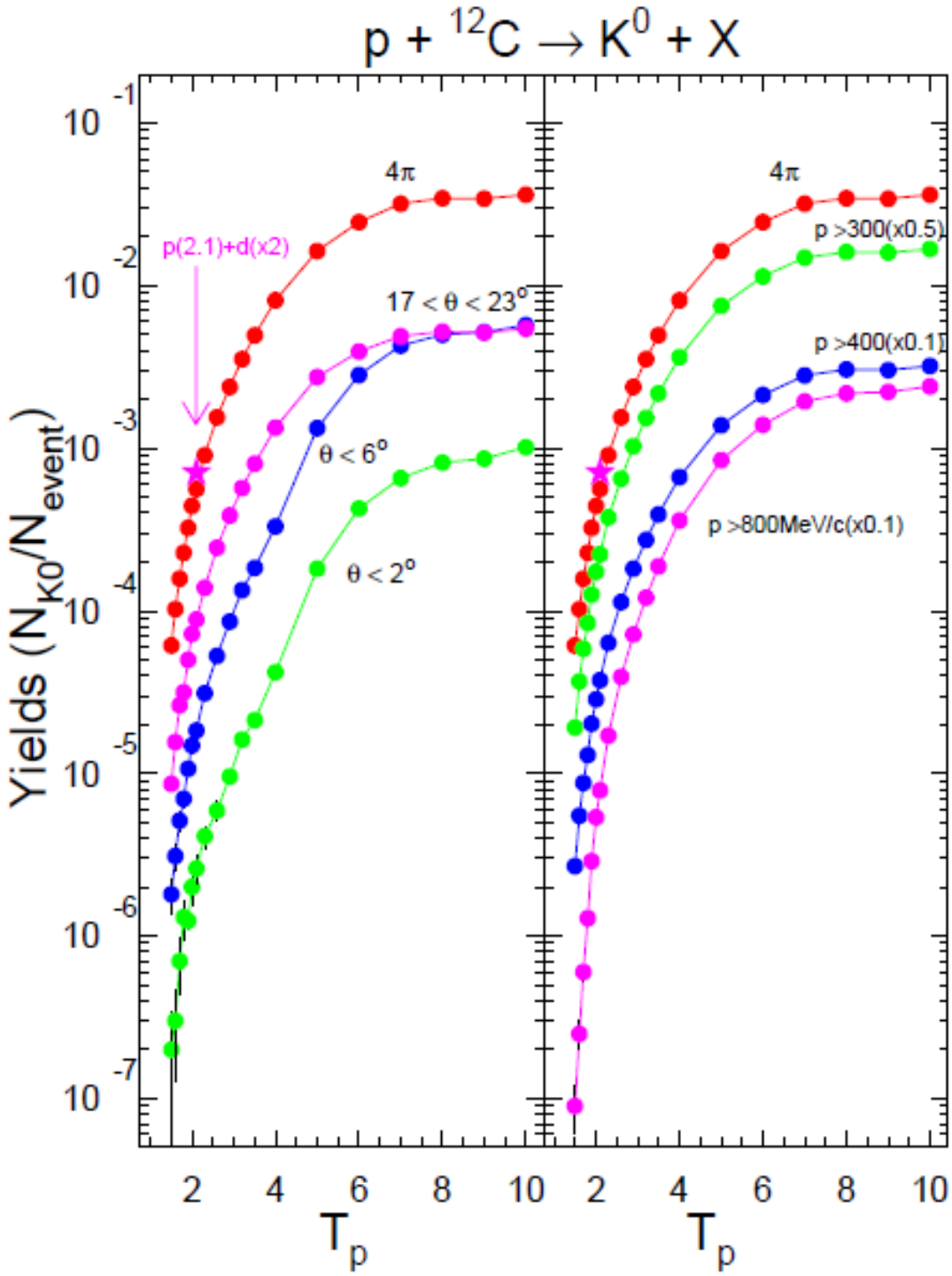

Figure 11. LAQGSM K_L yield as a function of T_p (GeV), kaon momentum and angles.

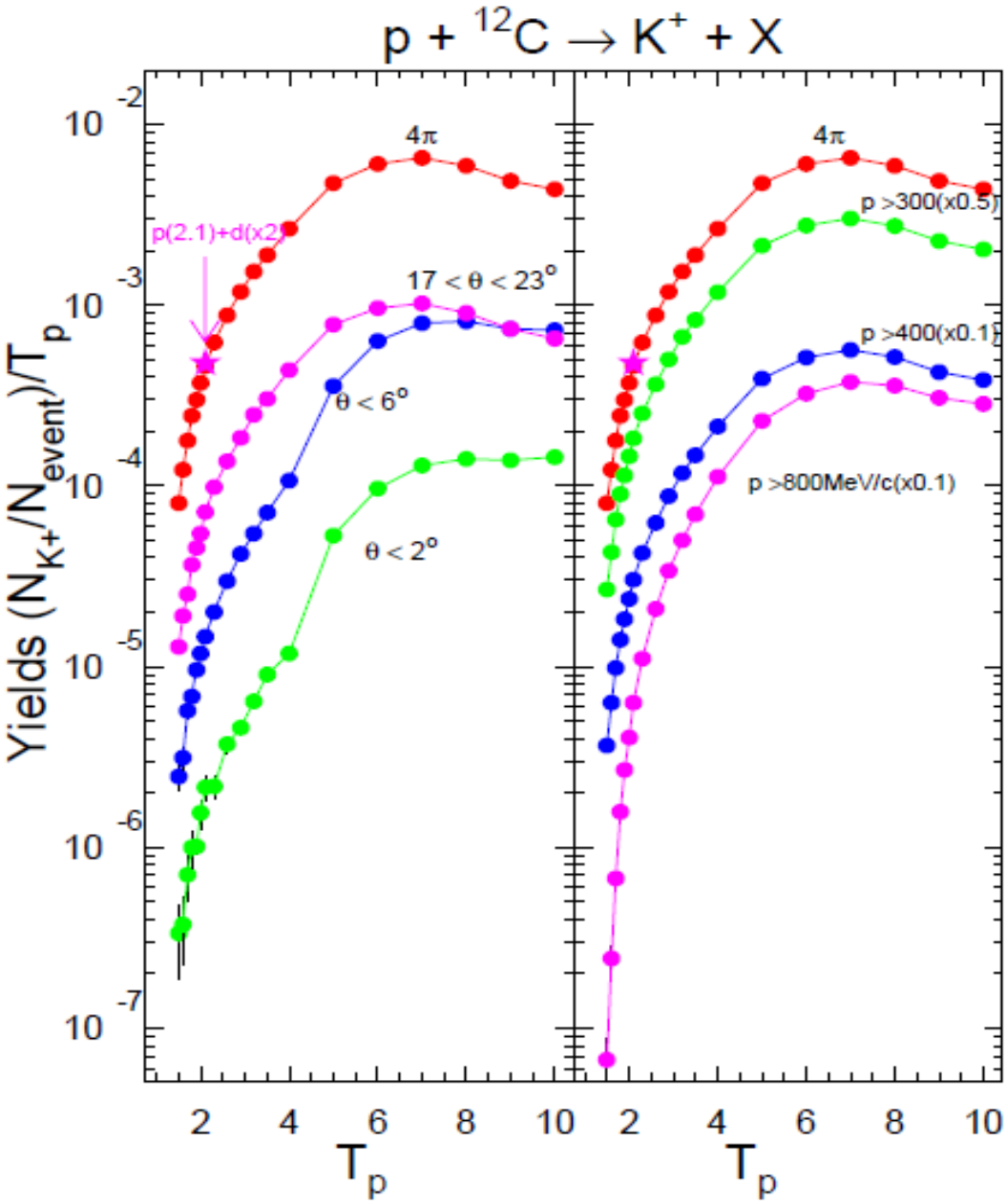

Figure 12. LAQGSM K^+-yield /T_p as a function of T_p (GeV), kaon momentum and angles.

Figure 12 shows that the kaon yield at constant beam power (yield/T_p) on carbon saturates at about 5 GeV, and the 2.1-2.6 GeV T_p range is a factor of about x4 less than the peak yield in the experimentally optimal angular region of 17-23 degrees. Despite this unsaturated yield there are in principle experimental advantages for producing kaons just above the threshold of associated (Λ,Σ) production channels. Strangeness is conserved in the production of kaons, and the associated hyperon can be useful in tagging in moderate rate experiments. The few-body kinematics such as $p^+n \rightarrow p^+\Lambda K^0$ could also be exploited to constrain the momentum of produced neutral kaons. In addition, below the K^-

production threshold indicated (2.6 GeV T_p) in figure 8 only K^0 neutral kaons are produced which can be useful tagging constraint in next generation interference experiments including CP, T, CPT and $K_L,K_S \rightarrow \pi^0 e^+ e^-$, $\pi^0 \mu^+ \mu^-$ studies.

Kaons can also be produced with a secondary π^- drive beam from the $\pi^- p^+$ total cross section as shown in Figure 6. The $\pi^- p^+ \rightarrow K^0 \Lambda$ exclusive reaction has particularly well constrained kinematics with a π^- drive beam near 1 GeV. This concept for driving a $K_L \rightarrow \pi^0 \nu\nu$ experiment was explored by Akira Konaka (TRIUMF) in the 1990s but was not published. The rates associated with this technique are discussed below.

The high ICD-2 beam current can compensate the reduced kaon production cross section near production thresholds. Further, the high duty factor and excellent time resolution of CW linac pinged beams would support unprecedented neutral kaon momentum resolution through TOF techniques developed by the KOPIO initiative [KOPIO reference XXX]. Experimental design concepts based on kinematically constrained beams and well established techniques developed for the BNL AGS implemented with ICD-2 are discussed in turn.

3.2.1 Concepts based on π^- drive beams:

For π^-s incident on a liquid hydrogen target with beam momentum below 1033 MeV/c the only strangeness producing reaction is $\pi^- p \rightarrow K^0,\Lambda$. Just above threshold ($\pi^-$ momentum ~ 900 MeV/c) the cross section for this reaction is about 0.1% of the total cross section, but the fraction rises to greater than 1% by ~980 MeV/c and is ~1.2% at 1033 MeV/c (threshold for $\pi^- p \rightarrow K^0,\Sigma^0$). Two body kinematics limit the range of K^0 momentum, and the Q of the reaction insures that a large fraction of the K^0_Ls have $\beta\gamma$~1. An initial MARS study of π^- production by a 2 GeV (kinetic) proton beam indicates that the yield of π^- with momentum in the range 950-1033 MeV/c is likely to be 4-7 π^- per 10,000 beam protons. The study assumed an 80 cm long carbon target and counted pions that crossed a 50 cm radius disc located 200cm downstream of the start of the target (subtending ~300 mrad from the center of the target). With default MARS settings, the yield of π^- in this momentum range was ~7×10^{-4}. The yield dropped to ~4×10^{-4} with the Los Alamos quark gluon string model option (LAQGSM). The pion momentum distribution is peaked at low momentum, but extends beyond 1.5 GeV/c and is essentially flat in the range 950 – 1033 MeV/c. Assuming a proton beam current of 1mA and the lower MARS estimate, but 100% efficiency for collection of π^-s within a 300 mrad cone, the π^- beam intensity would be 6×10^{15}/sec x 4×10^{-4} = 2.4×10^{12}/sec (2.8×10^{10}/sec per MeV/c).

The differential cross section for $\pi^- p \rightarrow K^0,\Lambda$ as a function of incident pion momentum was well measured in the 1960s and 70s. It is therefore straightforward to compute the yield and momentum spectrum of K^0_L as a function of angular acceptance for any assumed LH_2 target configuration and pion beam momentum spectrum. Table 3 gives the K^0_L rate for a range of angular acceptance assuming an 80 cm long LH_2 target and pion beam with a flat momentum distribution of 2.8×10^{10}/sec per MeV/c.

Incident π- Momentum	50 mrad	100 mrad	200 mrad	300 mrad
980 – 1020 MeV/c	13 MHz	48 MHz	170 MHz	395 MHz
950 – 1033 MeV/c	25 MHz	93 MHz	331 MHz	656 MHz

Table 3: K^0_L production rate into angular acceptance indicated.

Figure 13 shows the momentum spectrum of K^0_L produced into a forward cone of 200 mrad by a pion beam with a flat momentum spectrum between 980 and 1020 MeV/c.

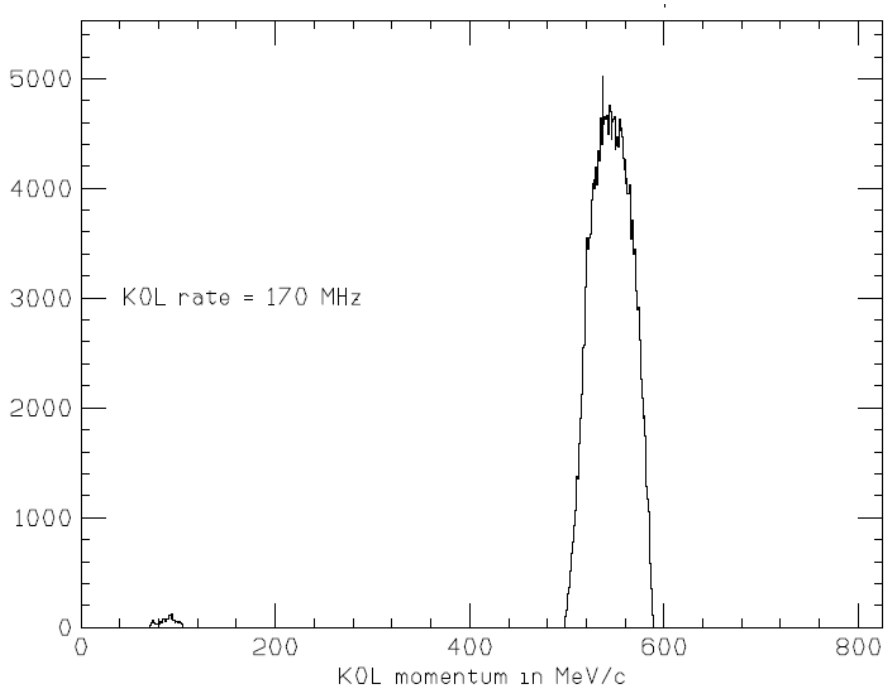

Figure 13. K_L Momentum distribution from $\pi^- p^+$ interactions on LH_2 .

The tertiary K_L beam produced by the secondary π^- beam has a well constrained momentum distribution and a relatively high purity (K_L/neutron > 1:30). The tertiary beam technique however comprises the K_L rate. All previous, current, and future experiments to search for and measure $K^0_L \rightarrow \pi^0\nu\nu$ are based on small solid angle beams less than 500 μsr. Probing this process to the Standard Model branching fraction of 3×10^{-11} is likely beyond the reach of the tertiary beam technique with such narrow beams. Nevertheless the relatively moderate neutron environment and tightly constrained K_L momentum distribution would benefit next generation precision interference measurements that exploit the well defined K^0 initial state.

3.2.2 Concepts based on "4π" detector geometries:

Figures 10 and 11 show the yield of charged and neutral kaons is about 0.2% per proton interaction for 2.1-2.6 GeV T_p protons on carbon. In this T_p range every kaon is produced in association with a hyperon. An open geometry "*4π*" experiment can be envisioned with a thin carbon target foil (1–5 μm, ~(2-10)x10^{-6} λ_I,) in the beam or possibly a hydrogen gas jet to minimize nuclear effects. At T_p = 2.6 GeV the (anti-K)/K production ratio on carbon is about 2% arising from intra-nuclear re-scattering, such as $\pi^-\Lambda^0 \rightarrow K^- n$, and Fermi-motion that raises the effective T_p above the (K,anti-K) production threshold. Both these sources of anti-K vanish with a hydrogen gas jet target at T_p < 2.6 GeV.

These gossamer targets could be instrumented with a solenoid-based detector system which could make precision measurements of many rare kaon and hyperon decay processes from the >20 MHz kaon and hyperon production rate. The interaction rate can be further reduced with thinner targets as needed to keep detector rates at a tolerable level. As noted previously in this T_p range only K^0 (and not anti-K^0) can be produced. This tagging constraint can be powerful in next generation interference measurements to probe CP, T, and CPT symmetries to unprecedented levels, and measure interference in important rare channels such as $K_S,K_L \rightarrow \pi^0 e^+ e^-$, $\pi^0 \mu^+ \mu^-$. This rate of tagged K^0 (and hyperons) is more than x10,000 the tagged pure K^0 rate from previous neutral kaon experiments (CPLEAR, where the K^0 yield/interaction was likewise 0.2%) and much greater than the $\phi \rightarrow K_S,K_L$ tagged kaon sample from KLOE.

3.2.3 Next generation $K \rightarrow \pi\nu\bar{\nu}$ experiments:

The 2008 Project-X workshops identified $K \rightarrow \pi\nu\nu$ experiments (Standard Model branching fractions of (3-7)x10^{-11}) with 1000 Standard Model event sensitivity as attractive goals of a new high power proton accelerator. Achieving this level of experimental sensitivity requires on the order of 10^{16} kaon decays in small solid angle beams. Two experimental approaches have been developed and extensively studied to drive $K \rightarrow \pi\nu\nu$ experiments with low-energy kaons: The BNL E787 & E949 experiments that discovered and established [E787/E949 XXX refs] the $K^+ \rightarrow \pi^+\nu\nu$ process and the KOPIO initiative [KOPIO XXX proposal] to discover and measure $K^0_L \rightarrow \pi^0\nu\nu$. Driving these well studied techniques with ICD-2 will be discussed in turn.

3.2.3.1: Next generation $K^+ \rightarrow \pi^+\nu\nu$ experiments:

The BNL E787/E949 program was the culmination of a long program of "stopping K^+ decays" experiments where a high flux low-energy K^+ beam is transported to a target where the K^+ stop and subsequently decay with a lifetime of 12 nsec. The beam that impinges on the stopping target must be primarily kaons in order to control detector rates. Achieving this beam purity requires a separator system to remove the overwhelming pion component. Balancing the lifetime of K^+ ($\beta\gamma c\tau$ ~ 3.5m) with the practical minimal length of a separator system (~14m) optimizes the separated beam momentum in the 500-

600 MeV/c range which fortuitously is maximally produced in ICD-2 as shown in figure 9. The secondary beam separator system for the BNL E787/E949 program is shown in figure 14 and the detector surrounding the active stopping target is illustrated in figure 15.

The BNL E949 experiment was not rate limited and this demonstrated performance serves as a good basis to sensibly extrapolate the reach of a high statistics experiment driven with ICD-2 beam. Studies initiating with the 2008 Project-X workshop suggest that the rate capability and acceptance of stopped K^+ technique can be further improved with straightforward detector upgrades and lowering the kaon momentum on the stopping target from 710 MeV/c to 550 MeV/c. A comparison of stopping rates is shown in table 4.

The "Tevatron Stretcher Initiative" listed in table 4 is a stopping K^+ experiment concept driven by high-duty factor 150 GeV beam extracted from the Tevatron after RunII. This stopped K^+ experiment concept is modeled closely after BNL E949 and projects a potential sensitivity of 100-200 Standard-Model $K^+ \rightarrow \pi^+ \nu\nu$ events per year. With 1/3 of the ICD-2 beam this reach could be extended by an order of magnitude beyond the Tevatron Stretcher Initiative. Remarkably, the ICD-2 stopping K^+ flux is 25% higher per watt (beam-power) than 150 GeV beam on the thick platinum target. A next generation experiment driven by ICD-2 will however have to deal with a much higher pion flux on the separator system, and there are plausible concepts being explored to control this fierce pion flux. .

	Beam Energy T_p	Protons/second (avg) on [target (λ_I)]	$p(K^+)$ (MeV/c)	Stopping K^+/second	K^+/π^+ Ratio
BNL AGS (E949)	21 GeV	12×10^{12} on [0.7 λ_I Pt.]	700-730	0.7×10^6	1:24
Tevatron Stretcher Initiative [Ref XXX]	150 GeV	3.6×10^{12} on [1.1 λ_I Pt.]	530-570	$(2\text{-}5) \times 10^6$	1:20
ICD-2	2.6 GeV	1/3 x 6000×10^{12} on [1.0 λ_I C]	530-570	43×10^6	1:120

Table 4: Compares the measured rate of stopping K^+ in the BNL-E949 experiment with full LAQGSM/MARS thick-target simulations for stopping rates in the Tevatron Stretcher Initiative and an identical beamline and stopping target with 1/3 of the ICD-2 beam power.

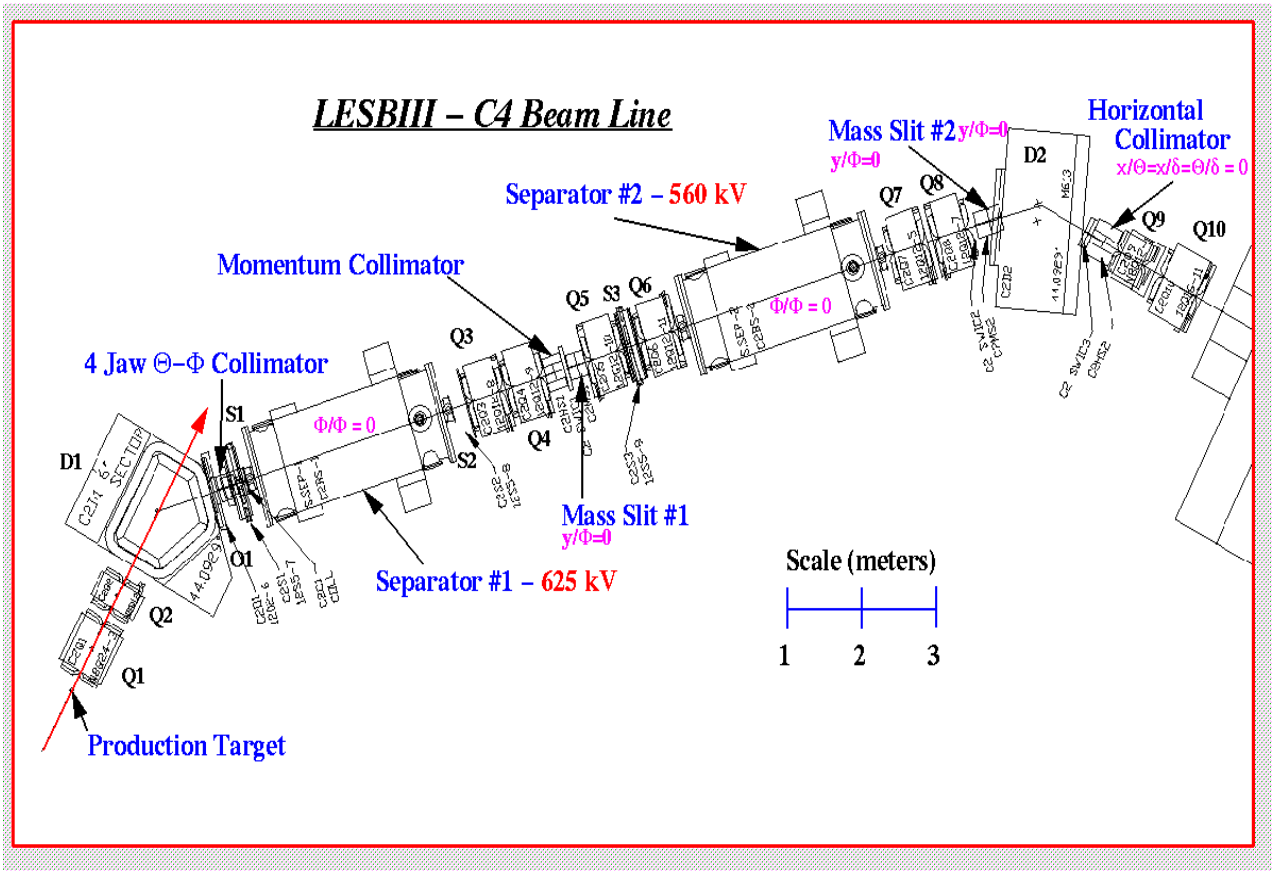

Figure 11: The Low Energy Separated Beamline (LESB) that collected, purified, and transported K^+ to the stopping target within the detector. The beamline operated at 710 MeV/c for E949 and delivered a K^+/π^+ purity of 3:1.

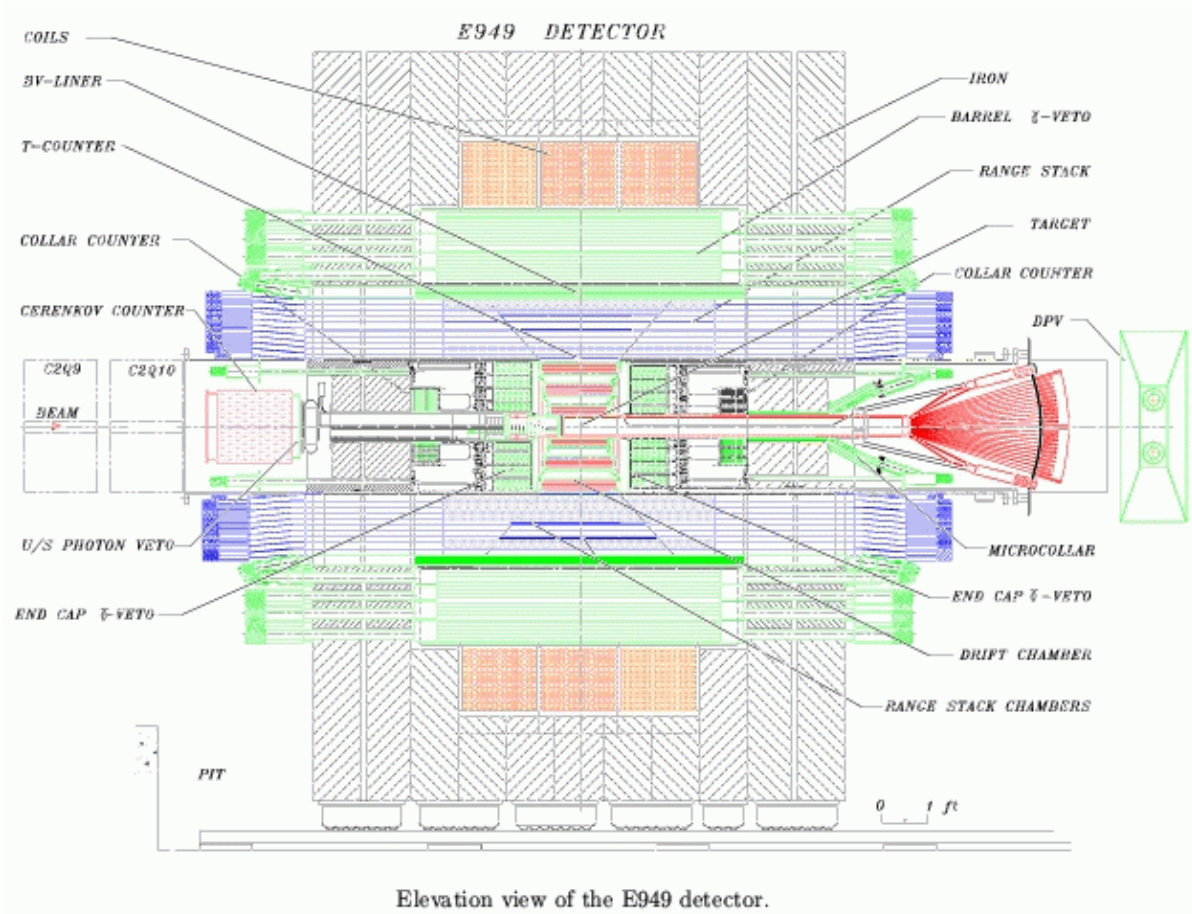

Elevation view of the E949 detector.

Figure 15: The E949 detector system surrounding the instrumented stopping target.

3.2.3.2: Next generation $K^0_L \rightarrow \pi^0 \nu\nu$ experiments:

The KOPIO initiative [Refs] proposed to measure the $K^0_L \rightarrow \pi^0\nu\nu$ process with a Standard Model sensitivity of 100 events. The experimental sensitivity required about 10,000 hours of BNL AGS proton beam upgraded to 100×10^{12} 24 GeV protons every 5 seconds. The neutral beam incident on the KOPIO detector was designed with a large angle ($\theta = 42^0$) from the production target in order to produce the low momentum neutral kaons critical to the Time-Of-Flight (TOF) strategy of the experiment. An illustration of the experimental technique is shown in figure 16. This K_L beam has an average kaon momentum of 800 MeV/c with ~1000 neutrons (E_n>10 MeV) for every K_L in the beam acceptance which requires that the beam propagate through an excellent vacuum. In the KOPIO design the kaon momentum is measured with TOF techniques in the 300-1200

MeV/c momentum range, which is well matched to the ICD-2 kaon momentum spectrum shown in figure 9. The projected TOF performance of KOPIO at the AGS was limited by achievable proton beam bunching of the AGS. Low intensity AGS beam-bunching test runs achieved a bunching of $\sigma_t \sim 270$ psec, with a design goal of $\sigma_t = 200$ psec. The ICD-2 beam bunching, including target time slewing, is expected to be less than 50 psec which would substantially improve the momentum resolution and background rejection capability of an experiment driven with ICD-2 beam. The comparative K_L production yields from thick targets fully simulated with LAQGSM and MARS are shown in Table 5.

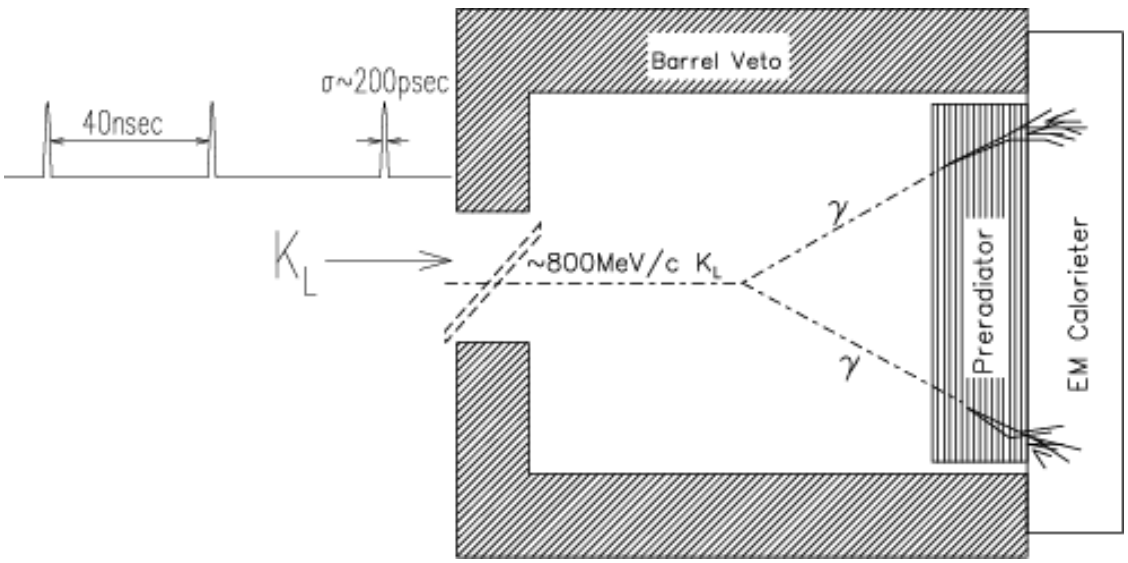

Figure 16: Illustration of the key elements of the KOPIO technique: TOF measurement of the K_L momentum, measurement of $(\pi^0 \rightarrow \gamma\gamma)$ and veto of all other background process particles.

	Beam Energy	Target (λ_I)	$p(K^+)$ (MeV/c)	K_L Yield (into 500 μsr)	K_L/n Ratio (E_n>10 MeV)
BNL AGS	24 GeV	1.1 Platinum	300-1200	$30x10^{-7}$ K_L/p	~1:1000
ICD-2	2.6 GeV	1.0 Carbon	300-1200	$1x10^{-7}$ K_L/p	~1:4000

Table 5 Comparison the K_L production from thick targets fully simulated with LAQGSM and MARS into the KOPIO beam and momentum acceptance. The BNL AGS kaon and neutron yields are from RSVP reviews in 2004 (Bryman) and Jaffe (2005).

Table 5 shows that the AGS K_L/p yield is x30 the ICD-2 K_L/p yield. ICD-2 can compensate with a proton flux x300 the AGS RSVP goal of $100x10^{12}$ protons every 5 seconds. Hence the ICD-2 neutral kaon flux into the KOPIO beam acceptance is x10 the AGS flux goal into the same beam acceptance. The KOPIO initiative had a statistical sensitivity of 100 Standard Model events with about 10,000 hours of running. A nominal five-year run with ICD-2 is x2.5 the duration of the KOPIO AGS initiative and hence the reach of an ICD-2 KOPIO experiment is x25 times the reach of the RSVP goals. An experiment based on 40% of the ICD-2 CW beam flux could have a sensitivity of 1000 Standard Model events with comparable detector rates of the AGS KOPIO design.

A TOF-based $K_L \rightarrow \pi^0\nu\nu$ experiment driven with ICD-2 would need to be re-optimized for the ICD-2 K_L momentum spectrum, TOF resolution, and corresponding background rejection. Nevertheless it is plausible that a $K_L \rightarrow \pi^0\nu\nu$ experiment based on the well studied KOPIO techniques could have ~1000 Standard Model event sensitivity.

3.2.4: ICD-2 operating energy for next-generation kaon experiments.

Figure 17 shows the dependence of kaon yield at constant beam-power as a function of T_p for the $K \rightarrow \pi\nu\nu$ experiments described in sections 3.2.3.1 and 3.2.3.2 . The maximum yield plateau at constant beam-power is $4<T_p<6$ GeV. Absent other considerations this would be the optimal operating range for these experiments. However the beam-current requirements of the neutrino program (LBNE) and ICD-2 facility costs that do not scale with beam power are important driving factors that push the optimal facility linac T_p below 4 GeV. The opportunity to mount an interesting program of interference experiments driven from a pure K^0 source outlined in section 3.2.2 is a further consideration that optimizes T_p near 2.6 GeV. As discussed in sections 3.2.3.1 and 3.2.3.2 a linac T_p operating point of 2.6 GeV is an excellent opportunity to deliver a 1000 event measurement of $K^+\rightarrow\pi^+\nu\nu$ and a plausible opportunity to measure $K^0_L \rightarrow \pi^0\nu\nu$ with high precision even though the corresponding yields are 1/3 of the optimum yield point.

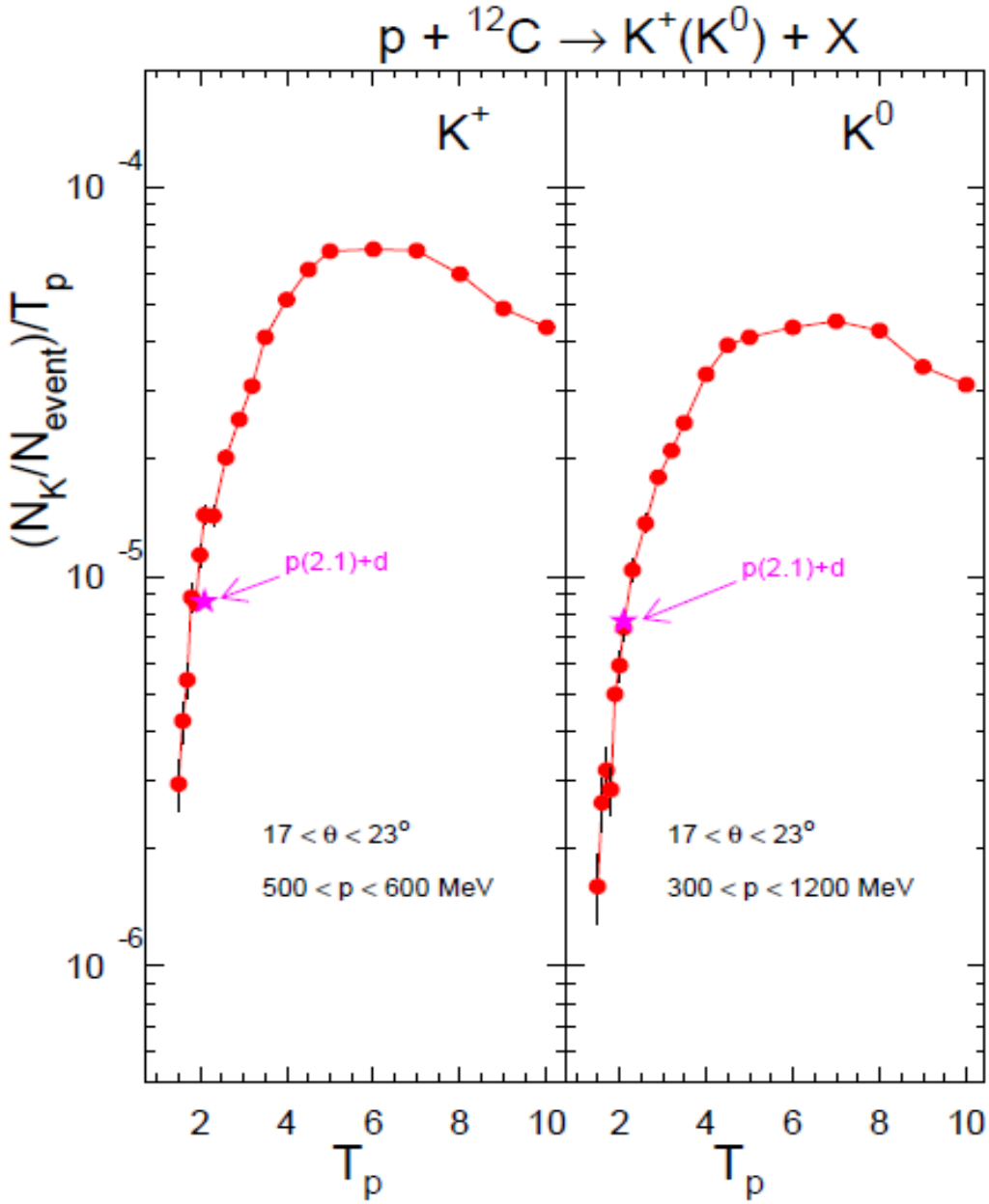

Figure 17: The K → πνν experiment (3.2.3.1 and 3.2.3.2) K^+ and K_L yields at constant beam-power as a function of T_p (GeV).

3.2.5 High duty factor kaon beams driven by the Tevatron stretcher

As previously noted the Project-X rare-decay program benefits greatly from high duty factor drive beams. The use of the Tevatron in the post-RunII era as a stretcher ring to condition Main Injector pulses into beams with nearly 100% duty factor has been studied [10] and is discussed in some detail in Appendix III. Configuring the Tevatron stretcher to accept 10% of the Main Injector beam power would provide a slow extraction beam facility in excess of the beam power achieved at the BNL AGS (which holds the world record in SEB power) but with much higher duty factor. Initial studies based on the K^+ production yield from the 120 GeV Tevatron Stretcher suggest that a 1000 event $K^+ \rightarrow \pi^+ \nu\nu$ experiment based on the demonstrated BNL stopping beam technique (BNL-E949, [11]) is plausible and further detailed studies are continuing. A new technique based on in-flight decays developed by the CKM experiment [12] could likewise exploit the Tevatron stretcher beam to plausibly achieve a 1000 event $K^+ \rightarrow \pi^+ \nu\nu$ experiment. Splitting and sharing beam between multiple experiments in a 120 GeV program would be straightforward, and such a program could include the E906 Drell Yan experiment and driving the test-beam facility which would both greatly benefit from high duty factor beams.

Appendix I

Charge:

The laboratory is now developing a conceptual design for the Project-X accelerator complex required to drive the research program described in the Project-X Initial Configuration Document (ICD, http://projectx.fnal.gov/): The elements of that research program are:

A neutrino beam for long baseline neutrino oscillation experiments. A new two or more megawatt proton source with proton energies between 50 and 120 GeV that would produce intense neutrino beams, directed toward a large detector located at a distant underground laboratory.

Kaon and muon based precision experiments driven by high intensity proton beams running simultaneously with the neutrino program. These could include a world leading muon-to-electron conversion experiment and world leading rare kaon decay experiments.

A path toward a muon source for a possible future neutrino factory and, potentially, a muon collider at the Energy Frontier. This path requires that the new proton source have significant upgrade potential.

The accelerator complex defined in the ICD can drive the long-baseline neutrino program, but does not readily provide a platform to pursue a research program in rare muon and kaon decays which requires high duty-factor proton beams.

As part of the standard DOE review process the Project-X design team is considering Alternate Conceptual Designs (ACDs) that can meet the research goals of the eventual Mission Need statement. Some of these ACDs may be more readily suited than the ICD The Project-X Research Program Task Force is charged to evaluate if and how the ICD and the ACDs can meet the research goals and recommend what R&D is necessary to refine the Project-X specifications required to drive the research program.

Appendix II:

Task-Force members:

D. Bryman	UBC/TRIUMF, Canada
M. Campbell	Michigan
D. Christian	Fermilab
P. Cooper	Fermilab
D. Glenzinski	Fermilab
K. Gollwitzer	Fermilab
K. Gudima	Institute of Nuclear Physics, Moldova.
Y. Kuno	Osaka, Japan
V. Lebedev	Fermilab
N. Mokhov	Fermilab
S. Nagaitsev	Fermilab
J. Peoples	Fermilab
S. Striganov	Fermilab
M. Syphers	Fermilab
R. Tschirhart	Fermilab (chair)
Y. Wah	Chicago

Appendix III

Remarks from the June 2009 Aspen Meeting of the Fermilab PAC:

Project X and ICD-1&2

The broad research program of Project X described in the "Golden Book" includes long-baseline neutrino experiments, neutrino interaction experiments, ultra-rare muon and kaon decay experiments, quark flavor experiments, and experiments with antiprotons. The Committee strongly recommends that Fermilab include budget estimates for the highest priority projects, such as muon-to-electron-conversion, $K^+ \to \pi^+ \nu \bar{\nu}$, and $K_L^0 \to \pi^0 \nu \bar{\nu}$ experiments, in the budgetary planning for Project X in order to insure a broad initial program of high-impact intensity frontier physics.

The long-baseline neutrino experiments and rare-decay experiments benefit most directly from the high beam power afforded by Project X. Although the design of the Project X accelerator complex described in ICD-1 provides for the beam power required for the long-baseline neutrino program, the high beam power produced at 8 GeV is not readily available for a full rare-processes program. As a result, the accelerator group is considering ICD-2 based on a 2 GeV CW linac containing some ILC-like modules, providing both higher beam power and a more flexible beam distribution scenario for the rare-processes program. This would be followed by a 2-8 GeV accelerating section similar to the SC linac of ICD-1 or a rapid-cycling synchrotron. This combination can provide great prospects for satisfying the broad goals of Project X. The ICD-2 can drive the long-baseline neutrino program while also providing nearly ideal beams for the important Project X rare-processes research program.

The ICD-2 concept is extremely promising. The Committee strongly endorses further study of the prospects to realize the great potential of the high-sensitivity studies of rare muon and kaon processes which will be essential elements of the intensity frontier explorations of new physics at high mass scales. The Committee strongly encourages Fermilab to further develop the accelerator aspects of this proposal, including cost considerations, and to continue to consider the synergy with the ILC linac technology. The Committee supports further detailed studies of the ICD-2 kaon and muon beams to confirm their suitability for next generation experiments.

Appendix IV

Opportunities and Issues of the 120 GeV Tevatron stretcher and 800 GeV operation.

As discussed in Ref [10], the Tevatron could be used quite readily as a "stretcher ring" for 120 GeV Fixed Target operations to the existing Fermilab Switchyard. Operation at 150 GeV, the Tevatron's design injection energy, could also be considered, but 120 GeV would allow for the use of standard NOvA-type cycles for the Main Injector. For example, assume the 1.333 s cycle time for the Main Injector that will be used for NOvA operation. With slip stacking employed, this will deliver 12 pulses from the Booster at approximately 4 Tp each, or 48 Tp into the Main Injector. As two MI pulses fill the Tevatron, one can envisage up to nearly 100 Tp stored in the Tevatron and slowly spilled using resonant extraction. The SY120 beam line set up could, in principle, be used "as is" or, if deemed necessary, the extraction point from the Tevatron can be moved to its original A0 location.

To investigate the range of possible operating scenarios, envision using 2 MI cycles out of every n (n>1) for use in this "Tev120" operation, with the remaining n-2 cycles sent to NOvA. Slow spill would occur during n-1 cycles, as depicted in Figure 2. The duty factor for Tev120 would be (n-1)/n, and the macro-duty factor of NuMI/NovA operations would be reduced by a of factor 2/n. Table 1 shows the particle throughput and average beam power delivered to Tev120 for a range of values of n. For example, a 10% reduction in the NOvA macro-duty factor program would support a Tev120 program which could deliver approximately 70 kW with 95% duty factor over a 26.7 s cycle time to experiments and the MTest program. In the absence of NuMI/Nova operations the Tev120 program could conceivably take all of the MI beam, and deliver 700 kW with a 50% duty factor.

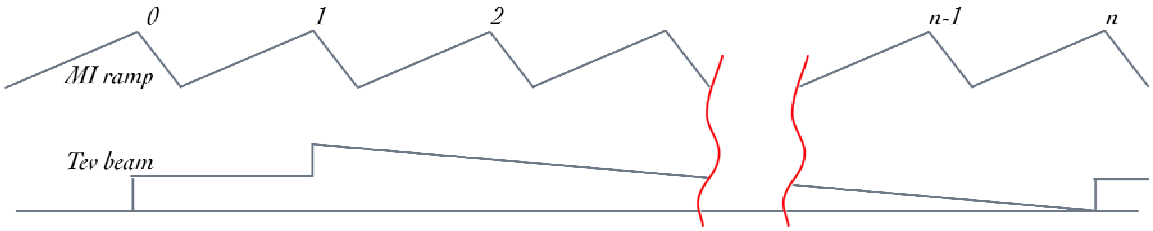

Figure 2. Main Injector energy ramps (top curve) and Tevatron beam intensity (bottom curve). Out of n, beam is injected over two cycles, and spilled for n-1.

n	T [s]	Duty factor [%]	NovA reduction [%]	P_{ave} [kW]	P_{max} [kW]	dN/dt_{Ave} [Tp/s]	dN/dt_{Max} [Tp/s]
2	2.667	50	100	691	1382	36.0	72.0
3	4.000	67	67	461	691	24.0	36.0
4	5.333	75	50	346	461	18.0	24.0
5	6.667	80	40	276	346	14.4	18.0
10	13.333	90	20	138	154	7.2	8.0
20	26.667	95	10	69	73	3.6	3.8
50	66.667	98	4	28	28	1.4	1.5
100	133.333	99	2	14	14	0.7	0.7
200	266.667	100	1	7	7	0.4	0.4

Table 1. Available power to Tev120 program and impact on Main Injector neutrino program. Here, beam is taken on two pulses out of *n* for TeV120. An initial Tevatron intensity of 96 Tp is assumed.

The Tevatron intensity used in the example above, ~100 Tp per pulse, was chosen as this is what the MI should be able to deliver. The record intensity achieved in the Tevatron during its fixed target history, however, was only approximately 30 Tp. The intensity was mainly limited then by beam instabilities at high energy, typically around 600 GeV. Additionally, the MI did not exist, and ~30 Tp was the limit that could be transferred from the old Main Ring injector. Operation at a constant 120 GeV, and improvements in beam feedback and damping systems, should allow for a much higher intensity throughput. For reference the Tevatron routinely delivered 64 kW (averaged over 60 seconds, 30% duty cycle) of 800 GeV extracted beam to experiments during the 1997 fixed target run.

Other items of note:

1) The existing A0 abort system can be used in this scenario, as 100 Tp @ 120 GeV is roughly equivalent to 12 Tp @ 1000 GeV.

2) Improvements made to impedances and to damper systems in the Tevatron during Run II would help with possible beam intensity-related instabilities.

3) The use of the existing F0 Lambertson magnet for both injection and extraction can be contemplated, which would require a polarity reversal switch. The electrostatic septum would then be placed in the C0 straight section, or at E48, and the existing SY120 beam line could be used, relinquishing the need to re-

establish the A0 extraction area. The QXR air core quadrupole system would be re-commissioned for tune feedback.

4) The beam is 2.5x larger at 120 GeV than at 800 GeV (for same emittance), so somewhat less aperture will be available for slow spill process.

5) A barrier bucket scheme can be employed to contain beam during injection and slow spill. Thus, no 53 MHz RF would be necessary (relinquishing these RF systems for possible use in MI/NOvA).

6) The Tevatron would be reconfigured to 1983 optics in long straight sections in order to lower the heat leak in the system and to improve extraction efficiency. The necessary magnetic elements are in storage.

7) As there will be no magnet ramping, no low-beta optics, and a lower operating current, there will thus be higher operating margin and more reliable operation of the magnet system.

8) The sextupole moment, b_2, at 120 GeV would be ~25% worse than at 150 GeV, potentially affecting chromaticity tuning, dynamic aperture, etc. However, b_2 drifts with time and would eventually reach its asymptotic value (toward zero). Thus, except following start-ups, etc., the dynamic aperture at 120 GeV should be not so different than at 150 GeV for Run II operation.

9) Operation of Tev120 would not affect the 8 GeV program whatsoever. Booster batches to fill MI on Tev120 cycles would be the same as on NOvA cycles. Thus, the same spare Booster cycles are still available for an 8 GeV program.

The main drawback of this scenario which immediately comes to mind is the operating cost of the cryogenic system and of the supporting infrastructure for the four-mile ring to support a 120 GeV fixed target program. The cost of running the Tevatron today is estimated at approximately $6-10M/year, not including labor to maintain the systems (perhaps up to ~$15M/year). Unfortunately, the fact that the power use of the Tevatron cryogenics system is dominated by the heat leak inherent in the magnets and in high temperature power leads, and the fact that the two-phase helium system cannot function above about 5°K prevent any savings from operating at a higher temperature with the present cryo equipment. However, power losses due to ramping would be avoided. Corrector circuits, which also produce a significant source of heat leak through their power leads, will be running at much reduced currents. The monthly power and cryogen M&S costs are expected to reduce from $710K/mo (collider operations) to $590K/mo (stretcher operations). Reduced demands on the RF system will also help the operational costs, and the reduced stress of all system components due to the DC operation should save maintenance costs. The main advantage of this program would be that it could easily come on line with very little additional up-front costs and with very little interruption to other laboratory operations. Since this proposal uses mostly already-

existing equipment, initiating this program would be straightforward and relatively low cost.

Tevatron 800 GeV Fixed Target

The Tevatron remains the world's only high energy (TeV-scale) synchrotron capable of rapidly ramping to full field and thus able to support a viable TeV-beam fixed target program. Although the fixed target operation was halted in 2000, the Tevatron is still capable of producing quality fixed target beams in the TeV energy range (800 GeV being the nominal high energy limit).

Using the scenarios described above, where beam intensities on the order of 50-100 Tp can be injected into the Tevatron from the Main Injector, and assuming that these intensities can be maintained to 800 GeV, a fixed target program with much higher throughput than in previous runs can be contemplated. Potential fixed target experiments at 800 GeV have been examined recently in both the charm and neutrino sectors [13] . One particular example is a high energy neutrino experiment proposed to Fermilab by the NuSOnG collaboration [14]. Here, a 40 s cycle time for the Tevatron and a 1 s flat top for fast extractions to the experiment have been suggested. Assuming the 1.333 s cycle time for the Main Injector, this would constitute a 2.667/40 = 6.7% impact on the running of the 120 GeV neutrino program from the MI. This Tevatron program would deliver an average of 250 kW of beam power at 800 GeV, and approximately 4×10^{19} POT/yr, assuming 80 Tp/pulse. NuSOnG, for example, would then reach its goal of 1.5×10^{20} within about 4 years of running.

To facilitate the return of a Tevatron 800 GeV fixed target program, in addition to the various items noted in the previous section, the C0 area beam abort would have to be re-commissioned and the extraction point would definitely need to be re-established at A0 (as there would not be room for 800 GeV extraction at F0, where the RF system is located). The necessary components for these all exist. Spare Tevatron magnets exist for running a fixed target program for 4-5 years, perhaps longer. Further details on reinstituting an 800 GeV program can also be found in [10].

Appendix V

Opportunities and Issues of Antiproton Source Operation

The existing Fermilab Antiproton Source can be easily used for an Accumulator based antiproton physics program after the conclusion of Run II. The only physical modification of the Antiproton Source would be to break Accumulator vacuum to install a detector. There are a few control issues that would have to be implemented since the CPU-network that communicated the deceleration commands was removed for Run II. In addition there would need to be several months to re-establish Accumulator deceleration ramps.

V.1 Antiproton Sources:

There are only two operating antiproton sources in the world. CERN operates the Antiproton Decelerator (AD) where the antiprotons are created every two minutes, captured and decelerated to very low energies. The extracted antiprotons are then used in several trapping experiments. CERN produces at most 3.5×10^{12} antiprotons each year. Fermilab operates the Debuncher/ Accumulator complex to produce antiprotons for the Tevatron collider program. During May 2009, 145×10^{12} antiprotons were produced; the stacking rate is $> 25 \times 10^{10}$ antiprotons per hour and routinely stacked to 10^{12} antiprotons.

A new antiproton source is proposed as part of the FAIR (Facility for Antiprotons and Ion Research) project that is to be hosted at GSI in Germany. The goal of the FAIR antiproton source is to stack at 3.5×10^{10} antiprotons per hour to a maximum of 10^{11} antiprotons. The FAIR project is to support both a trapping antiproton physics program as well as medium energy experiment with antiproton beam momentum between 1.5 and 15 GeV/c in a separate ring from the FAIR accumulation ring. The accumulation ring will spend half of its operation supporting the ion aspect part of FAIR as well. This means if FAIR achieves its goals, 95×10^{12} antiprotons per year will be available to the two antiproton physics programs.

V.2 Potential Accumulator Stacking:

After Run II, the Recycler will be recast as a proton accumulator which will allow one turn injection into the Main Injector. The ramp cycle time for the Main Injector to 120GeV will become 1.333s (currently at 2.2s due to having to load batches from 11 Booster cycles directly into the Main Injector). The future cycle time is too fast for the antiproton complex; therefore, antiproton production would be done every other Main Injector ramp cycle at 2.666s. Due to the relative size of the Antiproton Source rings to the Main Injector, only a fraction of the proton beam accelerated in the Main Injector is

used for antiproton production: currently 2 out of 11 Booster batches and in the future 2 of 12.

With the longer time between batches for antiproton production and going to larger stack sizes, we expect the stacking rate will average ~20×10^{10}. To support an antiproton physics program based in the Accumulator, stacking will be halted after collecting ~10^{12} antiprotons which are then decelerated to the momentum of interest (4 to 8.9 GeV/c has been achieved). If stacking, deceleration and data taking occur in a 24 hour cycle and roughly a quarter of that time is spent stacking, the reduction of protons for the NuMI/NoVa program will be (1/4 x 1/2 x 1/6) or ~2%. At 10^{12} antiprotons per day an Accumulator based program could use >200×10^{12} antiprotons per year. An Accumulator antiproton physics program will use more than twice the projected number of antiprotons at FAIR and the time frame will be 5 years before FAIR starts operation.

With a moderate increase to the gas jet target density that was used for E760/E835, a luminosity of 1-2×10^{32} $cm^{-2}s^{-1}$ is possible. Depending upon the beam energy, the beam lifetime will be 10-20 hours. With a 24 hour cycle to stack and take data, a program can expect to record ~8 pb^{-1} per day.

V.3 Unique Technique for Study of Charmonium and XYZ States:

The B-factories and collider experiments have center-of-mass energies much greater than the Charmonium or XYZ states. Much luminosity is expended at these higher center-of-mass energies and Charmonium and XYZ states are seen in low rate decays from these higher mass states. The data peaks observed are a convolution of a Briet-Wigner and the detector resolution for the overall decay channel being observed. The detector resolutions are mostly based upon Monte Carlo simulations and are very complicated. The typical detector resolution is a few MeV.

As shown by the previous Accumulator experiments E760/E835, the data peaks observed are a convolution of a Briet-Wigner and the beam distribution [1]. This is achieved since the antiproton beam energy width is small (a few hundred keV in the center-of-mass frame) and the beam energy is chosen such that the antiproton-proton annihilations sample a part of the Briet-Wigner resonance. The Accumulator is a spectrometer while the detector is a large scalar.

The beam energy is set and data are taken. The beam energy is changed and more data are taken. A scan across a state of interest is done. Electron-positron colliders can perform this technique only for $J^{PC} = 1^{--}$ states (for example J/ψ and ψ') while needing to make corrections for initial state radiation. Even though the 1^{--} states are as/more narrow than the antiproton beam distribution, the resulting de-convolution is straight forward and has resulted in the most precise measurement of the ψ' width [2] with many fewer events than the lepton colliders.

Once the peak of a resonance is established, the beam energy can be set to maximize the number of particles formed and studies of angular distributions and measurements of different low rate decays can be performed.

V.3.1 Example X(3872):

The X(3872) was discovered and confirmed after the last E835 run. X(3872) has been seen by Belle [3], CDF [4], D0 [5] and BaBar [6] in several channels: $J/\psi\ \pi^+\pi^-$, $J/\psi\ \pi^+\pi^-\pi^0$, $J/\psi\ \gamma$, and $D^0\ D^{*0}$. All measurements show that a resonance is narrow even though it is above the open charm threshold. In fact, mass determinations using the J/ψ channels and the D-state channel disagree with the former resulting in a mass less than the $D^0\ D^{*0}$ threshold. Are these the same particle or two resonances? An Accumulator scan of the resonance region counting inclusive J/ψ and the D-state channel will be able to resolve the resonance/resonances.

Since the range of masses reported for the X(3872) covers several MeV, an Accumulator scan using 0.25MeV steps over 10MeV will be necessary. Each scan point will take about a day. The branching fraction for formation of the X(3872) in antiproton-proton annihilation is not known, but it has estimated to be similar to the χ_c states. The decay rates are listed as seen except for $J/\psi\ \pi^+\pi^-$ being greater than 1% [7]. For E835, the number of events observed at the χ_{c0} peak was 30 events per pb^{-1} where the radiative decay to J/ψ is ~1% with no background. Within a factor of two, this is the number of events per pb^{-1} that would be expected at the X(3872) peak. Even if the production is down by an order of magnitude, the expected number of events for a day sitting on the peak will be a few tens of events. A two month scan triggering upon inclusive J/ψ and charmed particles could result in two distinct resonances. If needed, further scanning (smaller steps and/or more integrated luminosity per point) of the region could clarify the resonance(s). Sitting on the mass peak, the different branching fractions can be measured while measuring the angular distribution of the decay products.

V.3.2 Charmonium and other XYZ states:

The same technique can be used to scan the charmonium states η_c, h_c and $\eta_c^{/}$. The Accumulator's maximum beam energy corresponds to a center-of-mass energy about 4.3 GeV which allows the Accumulator to investigate at least six other XYZ states other than the X(3872).

References:

[1] Project-X ICD reference. (http://projectx.fnal.gov/)

[2] Golden book reference:
http://www.fnal.gov/directorate/Longrange/Steering_Public/P5/GoldenBook-2008-02-03.pdf

[3] C. Ankenbrandt et al., Mu2e Document 516. Mu2e and (g-2) websites:
http://mu2e.fnal.gov/,
http://www.facebook.com/pages/The-new-g-2-experiment-at-Fermilab/76812692423

[4] N.V. Mokhov, "The Mars Code System User's Guide", Fermilab-FN-628 (1995); N.V. Mokhov, S.I. Striganov, "MARS15 Overview", in Proc. of Hadronic Shower Simulation Workshop, Fermilab, September 2006, AIP Conf. Proc. 896, pp. 50-60 (2007);
http://www-ap.fnal.gov/MARS/

[5] S.G. Mashnik et al., "CEM03.03 and LAQGSM03.03 Event Generators for the MCNP6, MCNPX and MARS15 Transport Codes", LANL Report LA-UR-08-2931 (2008); arXiv:0805.0751v1 [nucl-th] 6 May 2008.

[6] http://www.fluka.org/fluka.php

[7] http://nds121.iaea.org/alberto/mediawiki-1.6.10/index.php/Benchmark:CalculRes

[8] H. En'yo et al., Phys. Let. B159, pp. 1-4 (1985).

[9] M.G. Catanesi et al., Phys. Rev. C77, 055207 (2008).

[10] M. Syphers, Beams-doc-2222, Beams-doc-2849. (http://beamdocs.fnal.gov)

[11] BNL E949 experiment website: http://www.phy.bnl.gov/e949/

[12] CKM experiment website: http://www.fnal.gov/projects/ckm/Welcome.html

[13] T. Adams, et al., "Renaissance of the ~1 TeV Fixed-Target Program,"
http://arxiv.org/abs/0905.3004 .

[14] T. Adams, et al., "Terascale Physics Opportunities at a High Statistics, High Energy Neutrino Scattering Experiment: NuSOnG," Int. J. Mod. Phys. A24: 671-717, 2009, also
http://arxiv.org/abs/0803.0354 .

CERN proton driver study reference:

CERN-TH/2001-175
hep-ph/0107046
July 2001

Optimized yield studies based on SW, 2-20 GeV kaons.

[M.1] See for example M. Raidal et al., Eur. Phys. J. C 57, 13 (2008) and references therein.
[M.2] C.Dohmen et al. (SINDRUM-II Collaboration), Phys. Lett. B 317, 631 (1993).
[M.3] W. Bertl et al. (SINDRUM-II Collaboration), proceedings from the International Europhysics Conference on HEP, http://www.hep2001.elte.hu/, (2001).
[M.4] R.M. Carey et al. (Mu2e Collaboration), Fermilab Proposal 0973 (2008).
[M.5] E. Prebys, "Mu2e Beamline Specifications", internal Mu2e-doc-74 (2008); see also Chapter X of Ref [M.4].
[M.6] S. Nagaisev and V. Lebedev, personal communication.
[M.7] H. Herzog and K. Alder, Helvitica Physica Acta 53, 53 (1980); O.Shankar, Phys. Rev. D 25 1847 (1982).
[M.8] The DIO fraction is $f_{DIO} = (1-f_{OMC})$, where f_{OMC} is the ordinary muon capture fraction taken from Ref [M.10].
[M.9] R. Watanabe et al., Atomic and Nuclear Data Tables 54, 165 (1993).
[M.10] T. Suzuki et al., Phys. Rev. C 35 2212 (1987).
[M.11] R. Eramzhyan et al., Nucl. Phys. A 290, 294 (1977).
[M.12] D. Bryman et al. (COMET Collaboration), J-PARC Proposal P21 (2007).
[M.13] RSVP Proposal, available at http://meco.ps.uci.edu/old/, (1999).
[M.14] For a recent description see A. Sato, "Status of PRISM-FFAG R&D", presented at the NuFact09 Conference, Chicago, IL (2009).
[M.15] C. Ankenbrandt, "Mu2e Upgrade Ideas for Project X Era", internal Mu2e-doc-497 (2009).
[M.16] M. Ahmed et al. (MEGA Collaboration), Phys. Rev. D 65, 112002 (2002).
[M.17] J. Adam et al. (MEG Collaboration), arXiv:0908.2594v1 [hep-ex] (2009).
[M.18] U. Bellgardt et al. (SINDRUM Collaboration), Nucl. Phys. B 299, 1 (1988).
[M.19] A. van der Schaaf, presentation at the CHIPP workshop (2008).
[M.20] T.E. Clark and S.T. Love, Mod. Phys. Lett. A 19, 297 (2004).
[M.21] A. Gusso, C.A. de Spires, and P.S. Rodriguez da Silva, J. Phys. G 30, 37 (2004).
[M.22] L. Willmann et al. (MACS Collaboration), Phys. Rev. Lett. 82, 49 (1999).
[M.23] G.W. Bennett et al. (Muon g-2 Collaboration), Phys. Rev. Lett. 92, 161802 (2004); ibid Phys. Rev. Lett. 89, 101804 (2002).

[M.24] For a recent discussion see M.Davier et al., arXiv:0908.4300 [hep-ph] (2009) or K. Hagiwara et al., Phys. Lett. B 649, 173 (2007).
[M.25] R.M. Carey et al. (New g-2 Collaboration), Fermilab Proposal 0989 (2009).
[M.26] N. Saito et al, http://meson.riken.jp/g-2/index.html
[M.27] P.A.M. Dirac. Proc. R. Soc. (London) **A117**, 610 (1928).
[M.28] B.C. Regan *et al*., Phys. Rev. Lett. **88** 071805-1 (2002).
[M.29] W.C. Griffith *et al*., Phys. Rev. Lett. **102**, 101601 (2009).
[M.30] J. Bailey *et al*., J. Phys. **G4**, 345 (1978).
[M.31] J.L. Feng, K.T. Matchev, Y. Shadmi, Nucl. Phys. **B 613**, 366 (2001).
[M.32] JPARC Letter of Intent L22, BNL Letter of Intent, Spring 2000, Y.K. Semertzidis *et al*., arXiv:hep-ph/0012087v1.

[V.1] T.A. Armstrong et al., Nucl. Phys. B373:35 (1992).

[V.2] M. Andreotti et al., Phys. Lett. B654: 74 (2007).

[V.3] S.K. Choi et al., Phys. Rev. Lett. 91:262001 (2003); G. Gokhroo et al., Phys. Rev. Lett. 97:162002 (2006).

[V.4] D. Acosta et al., Phys. Rev. Lett. 93:072001 (2004); T. Aaltonen et al., arXiv:0906.5218 submitted to Phys. Rev. Lett. (2009).

[V.5] V.M. Abazov et al., Phys. Rev. Lett. 93:162002 (2004).

[V.6] B. Aubert et al., Phys. Rev. D71:071103 (2005); B. Aubert et al., Phys. Rev. D77:011102 (2008); B. Aubert et al., Phys. Rev. Lett. 102:132001 (2009).

[V.7] C. Amsler et al., Phys Lett. B667:1 (2008) and 2009 partial update for the 2010 edition.